

## Localization of Neuropeptides in the Nervous System of the Brittle Star *Ophiura Ophiura*

M. Ghyoot, J. L. S. Cobb and M. C. Thorndyke

*Phil. Trans. R. Soc. Lond. B* 1994 **346**, 433-444  
doi: 10.1098/rstb.1994.0160

### Email alerting service

Receive free email alerts when new articles cite this article - sign up in the box at the top right-hand corner of the article or click [here](#)

To subscribe to *Phil. Trans. R. Soc. Lond. B* go to: <http://rstb.royalsocietypublishing.org/subscriptions>

# Localization of neuropeptides in the nervous system of the brittle star *Ophiura ophiura*

M. GHYOOT<sup>1</sup>, J. L. S. COBB<sup>1</sup> AND M. C. THORNDYKE<sup>2</sup>

<sup>1</sup>*Department of Biology, University of St Andrews, Fife KY16 8LB, U.K.*

<sup>2</sup>*Biology Department, Royal Holloway College, University of London, Egham, Surrey TW20 0EX, U.K.*

## SUMMARY

Immunocytochemical investigations using antisera against the SALMFamide neuropeptide S1 and RFamide were carried out on whole mounts of the radial nerve cord and circumoral ring of the brittle star *Ophiura ophiura*. Both antisera show an abundant immunoreactivity in the ectoneural tissue and give similar patterns of distribution. They show that in the radial nerve cord there are discrete populations of neurons organized in an identical pattern in each segment. At the junction with the ring, however, the two proximal segments of the nerve cord are differentiated from the distal ones by increased numbers of immunoreactive neurons. This is probably due to the more complex integrative function in that area. In the ring, immunolabelling is simple and consists of fibre tracts and two local ganglia. In each segment both antisera label either one or two giant neurons the shape of which is similar to that of a class of fibres that have been described from intra-cellular dyefills. The S1- and RFamide-like distributions, although very similar, show some neurons which are only labelled by one antiserum. Since preabsorption controls indicate no cross-reactivity between antisera, there is evidence of two distinct neuropeptides in the nervous system of the brittle star.

## 1. INTRODUCTION

It is only recently that attention has been paid to echinoderm neuropeptides. In particular, using an antiserum against the molluscan cardioexcitatory neuropeptide FMRFamide (Price & Greenberg 1977), immunoreactivity was detected in the nervous system of the starfish *Asterias rubens* (Elphick *et al.* 1989). Subsequently, two novel related neuropeptides, the SALMFamides, were isolated from the radial nerve cord of the starfishes *Asterias rubens* and *A. forbesi*. These are S1, an octapeptide with the amino acid sequence GFNSALMFamide, and S2, a dodecapeptide with the sequence SGPYSFNSGLTFamide (Elphick *et al.* 1991a). As no FMRFamide-related peptides (FaRPs) were detected in the starfish, the previously reported FMRFamide-like immunoreactivity was attributed to the SALMFamides (Elphick *et al.* 1991a). Specific antisera have been raised against S1 and the distribution of the neuropeptide has been reported in the nervous system of the starfish, *Asterias rubens*, and larval echinoid (Moore & Thorndyke 1993; Thorndyke *et al.* 1992, respectively). Its wide distribution in both classes indicates that SALMFamide neuropeptides have an important function in echinoderm neurobiology.

The nervous system of the brittle star *Ophiura ophiura*, particularly the radial nerve cord and the circumoral nerve ring, has so far been the most

studied of the echinoderms. This is because a population of giant cells has for the first time allowed intracellular recordings in echinoderms (Cobb 1985). The morphology and distribution of some neurons, as well as physiological activities correlated with behaviour, have been reported (Cobb 1985; Cobb & Ghyoot 1993). Although the neurobiology of brittle stars is better understood than in other classes of echinoderms, as yet nothing is known about the occurrence of neuropeptides or their function in these animals.

In an attempt to identify neuropeptide-containing neurons, we have carried out an immunocytochemical study on the distribution of S1-like immunoreactivity (S1-Li IR) in the radial nerve cord and circumoral ring of the brittle star *Ophiura ophiura*. In addition, we also have compared the distribution of S1-Li IR to that obtained with an antiserum raised against the RFamide sequence, which is common to all FaRPs.

## 2. METHODS

Neuropeptide distribution was investigated on both whole mount preparations and paraffin wax sections by using indirect immunocytochemical methods.

Specimens of *Ophiura ophiura* were obtained from the Marine Biological Station of Millport, Isle of Cumbrae. Segments of radial nerve cords and circumoral rings were fixed in 4% paraformaldehyde in 0.1 M phosphate buffer (pH 7.2) for 2 h at room

temperature and then rinsed in the same buffer for 30 min. For the sections, the material was embedded by routine methods in paraffin wax, sectioned at 8  $\mu\text{m}$  and mounted on poly L-lysine coated glass slides. Antiserum against S1 (BL IIIb) was raised in rabbits to the C-terminal pentapeptide analogue of S1, KYSALMFamide. This has a high affinity for S1 and KYSALMFamide and exhibits very negligible cross-reactivity to S2 and the FMRFamide-related peptides (FaRPs) (Elphick *et al.* 1991b). It should be noted, however, that Elphick *et al.* used an earlier bleed (BL II) but Moore and Thorndyke (1993) described the properties of a later one (BL IV). BL IIIb is intermediate in properties and this has been described by Elphick (1991). The antiserum against RFamide (146 III, Grimmelikhuijzen) was obtained by immunizing rabbits to synthetic RFamide; it recognizes peptides belonging to the family of the FaRPs (Grimmelikhuijzen 1985).

For whole mounts and sections, the fixed material was transferred for 1 h in PBS (pH 7.2) containing 0.25% Triton (PBS-Triton) and for 2 h in 20% donkey serum (SAPU) in the same buffer containing 0.1% BSA (PBS-Triton-BSA). Primary antisera were applied overnight (sections) and for 36 h (whole mounts) at room temperature using dilutions between 1:500 to 1:1000 in PBS-Triton-BSA containing 10% donkey serum. After several washes in PBS-Triton, the material was transferred for 2 h at room temperature to fluorescein isothianate (FITC)-labelled donkey anti-rabbit IgG second antiserum (SAPU) diluted 1:100 with PBS-Triton-BSA. Following three washes, the whole mounts and sections were mounted in buffered glycerol and examined with either a Leitz epifluorescence microscope or a confocal scanning laser microscope Bio-Rad MRC 600.

As controls, S1 antiserum was incubated with 10  $\mu\text{mol}$  of KYSALMFamide or S1 and with 100  $\mu\text{mol}$  of RFamide (Bachem)/ml of diluted antiserum; RFamide antiserum was incubated with 100  $\mu\text{mol}$  of RFamide and with 10  $\mu\text{mol}$  of KYSALMFamide or S1/ml of diluted antiserum. The binding of non-immune serum was also examined.

### 3. RESULTS

The nervous system of *Ophiura ophiura* consists of five radial nerve cords interconnected by five branches forming the circumoral ring (Cobb & Stubbs 1981, 1982). Essentially, the radial nerve cord, schematically illustrated in figure 1a, consists of a flattened ribbon of segments, each segment comprising a ganglion interconnected by an interganglion. It is composed of two superimposed tissues, the ectoneural and hyponeural, separated by a connective tissue layer. The ectoneural tissue is the most developed and is connected to the peripheral regions of the arm (tube feet, for example) by lateral branches. The hyponeural tissue is only apparent in the ganglia of the nerve cord and comprises motor nerves which innervate the intervertebral muscles.

At the junction with the ring, each nerve cord ends with a short segment (the first proximal segment) in

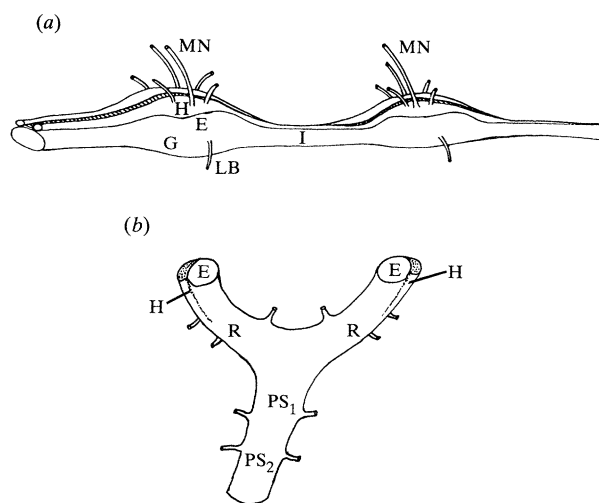


Figure 1. (a) Diagram of part of the radial nerve cord of *Ophiura ophiura*. The radial nerve cord consists of a chain of segments, each segment being made of a ganglion (G) interconnected by an interganglion (I). It is composed of two superimposed nervous tissues, the ectoneural (E) and the hyponeural (H). The ectoneural tissue sends lateral branches (LB) which supply the podia (not represented here). From the hyponeural tissue, motor nerves (MN) ascend aborally to innervate the intervertebral muscles (not represented here). (b) Diagram of the junction between the radial nerve cord and the ring in *Ophiura ophiura*. The proximal end of the radial nerve cord represented by the second (PS<sub>2</sub>) and the first (PS<sub>1</sub>) proximal segments is continuous with two ring branches (R). In each ring branch, the hyponeural tissue (H) lies on the outside of the ectoneural (E).

continuity with two ring branches running in opposite directions to the adjacent radii (figure 1b). The ring branches are round in profile and unlike the radial nerve cords do not show segmental ganglionic swellings. Here too, there are two separated nervous systems with hyponeural tissue lying on the outside of the ectoneural.

#### (a) S1-like immunoreactivity

S1-like immunoreactivity (S1-Li IR) was abundant in both the radial nerve cords and the circumoral ring and is illustrated schematically in figure 2. The excellent quality of the staining, especially in whole mount, made it possible to analyse precisely the pattern of distribution for each segment of the nerve cord and for the ring.

##### (i) The radial nerve cord

In the radial nerve cord, most of the immunoreactivity was located in the ectoneural tissue (figures 2a, 3). In the hyponeural tissue, immunoreactivity was only detected in a few axons running in the motor nerves (figure 4). In transverse sections of a ganglion, no labelling was observed in the hyponeural cell bodies (figure 3).

The distribution of S1-Li IR in the ectoneural tissue is schematically represented in figure 2a. S1 antiserum strongly labelled five distinct nerve plexuses parallel to

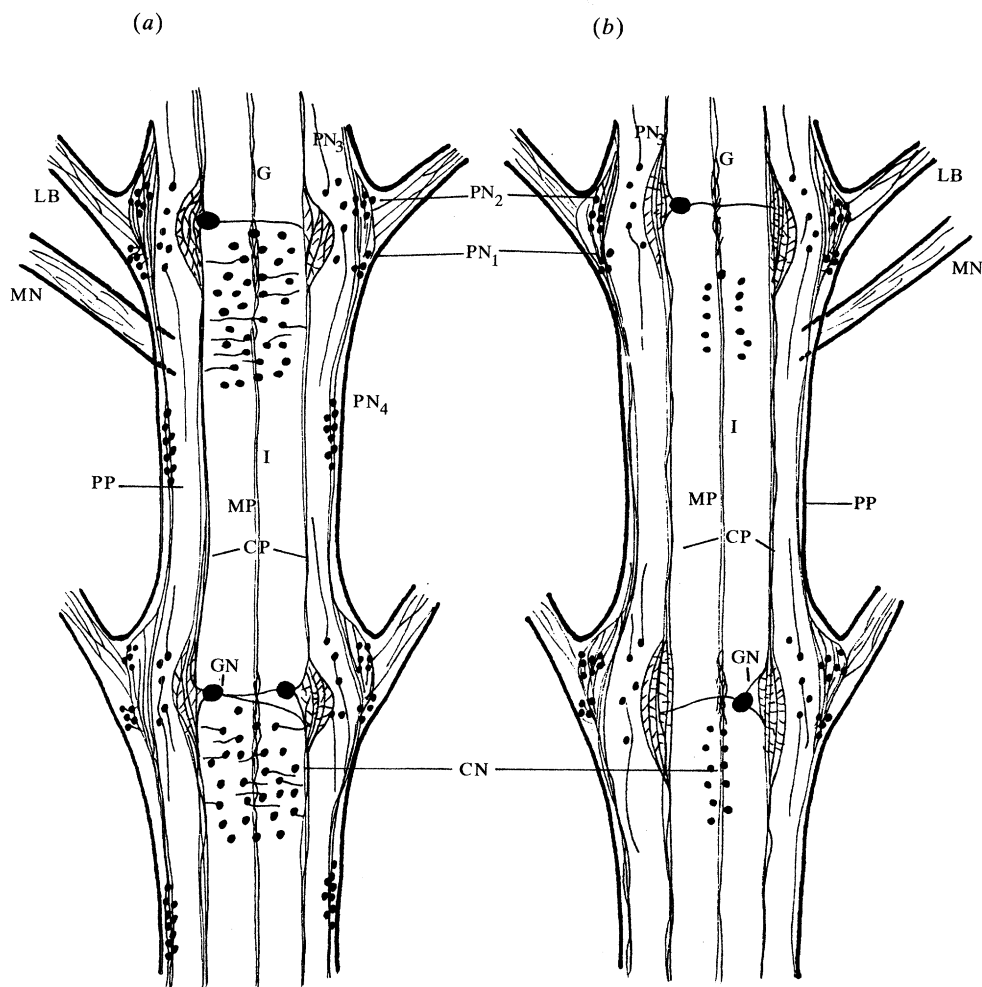


Figure 2. Schematic representation of the immunolabelling in the radial nerve cord of *Ophiura ophiura*. (a) S1-Li IR; (b) RFa-Li IR. There are in the ectoneural tissue five fibre plexuses: two peripheral (PP), two central (CP), and one median (MP). Four groups of immunoreactive neurons are found close to the peripheral plexuses: PN<sub>1</sub> and PN<sub>2</sub>, beside and at the base of the lateral branch (LB), respectively, PN<sub>3</sub> between the peripheral and the central plexuses, PN<sub>4</sub> in the interganglion (I). Between the central plexuses, there are in each ganglion (G), one giant neuron (GN) and adjacent to it, a population of small neurons (CN). The hyponeural tissue is only represented by a motor nerve (MN) which contains a few immunoreactive axons.

The comparison between *a* and *b* shows that in RFamide-like distribution, there are no peripheral neurons PN<sub>4</sub> in the interganglion and less central neurons CN between the central plexuses.

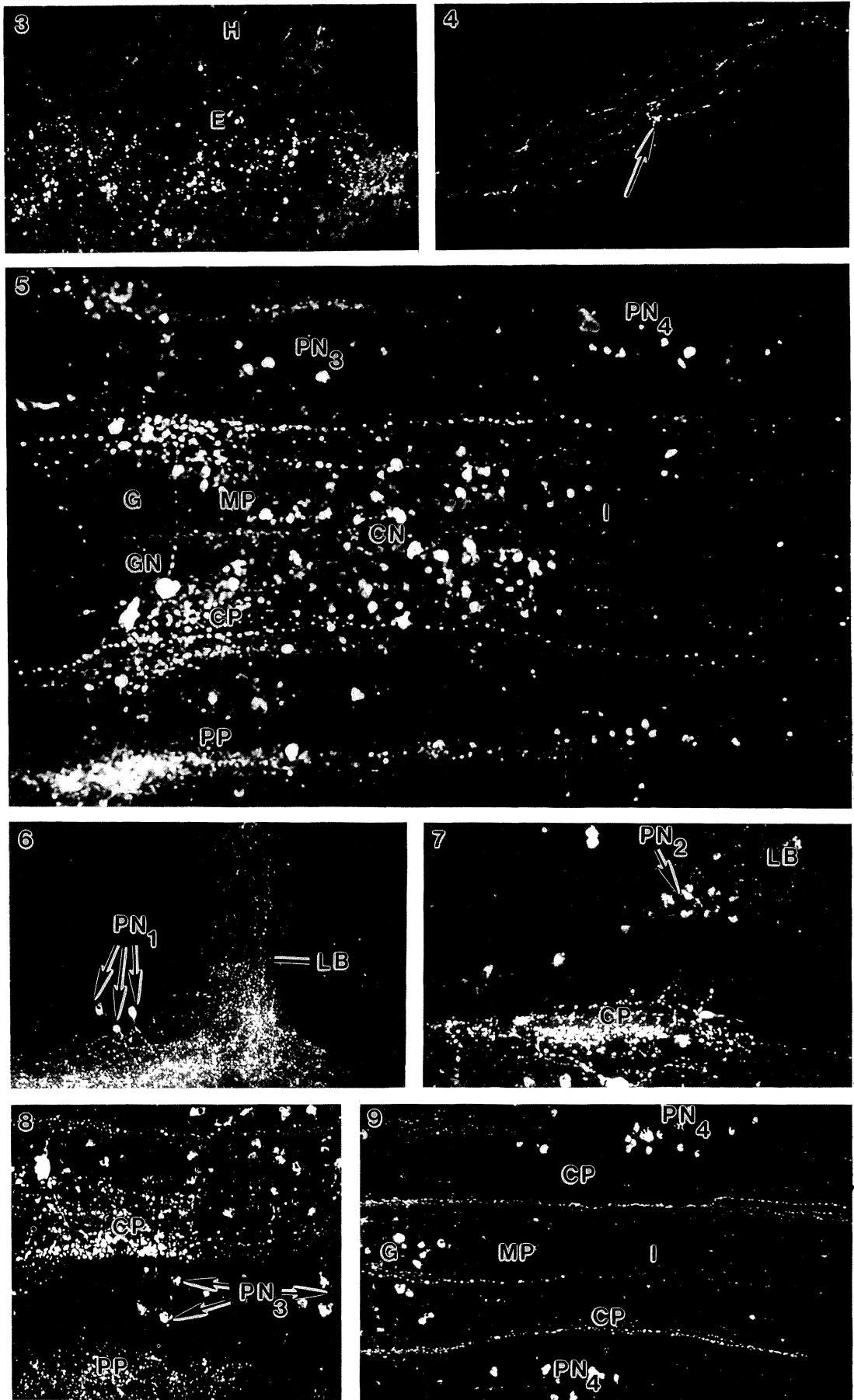
each other and running along the whole length of the nerve cord. There were two peripheral plexuses along the nerve cord edges (figures 2*a*, 5), one median along the midline (figures 2*a*, 5, 9), and two central, halfway between the peripheral and the median plexuses (figures 2*a*, 5, 9). Very few transverse connections were seen between the plexuses. Each plexus consisted of a meshwork of fine varicose fibres which were more densely packed in the ganglia than in the interganglia (figure 5). At the base of the lateral branches the peripheral plexuses showed an area of intense fluorescence which was in continuity with a nerve plexus running in each lateral branch (figure 6).

There were numerous immunoreactive cell bodies associated with the plexuses and always situated at the surface of the ectoneural tissue – as indeed are all cell bodies in ectoneural nerve cord (see Cobb & Stubbs 1981). The cell bodies occupied a precise position which was identical in each segment of the nerve cord except the proximal ones (see below). The cell bodies

were generally aggregated into clusters; they were of a small diameter (8–15 µm) and belong to monopolar or bipolar neurons.

Four distinct groups of neurons were found in, or in the vicinity of, each peripheral plexus. These were: (i) 4–6 bipolar neurons situated beside the lateral branch (PN<sub>1</sub>; figures 2*a*, 6); (ii) 10–15 monopolar neurons located at the base of the lateral branch (PN<sub>2</sub>; figures 2*a*, 7); (iii) 5–10 scattered bipolar neurons situated in the ganglion between the peripheral and the central plexuses (PN<sub>3</sub>; figures 2*a*, 5, 8); and (iv) 15–20 monopolar neurons in the interganglion (PN<sub>4</sub>; figures 2*a*, 5, 9).

Two types of immunoreactive neurons were detected in each ganglion between the central plexuses. The first type consisted of an extensive population (more than 70 neurons) of small monopolar neurons (cell body diameter *ca.* 15 µm) extending over the ganglion and part of the interganglion (CN; figures 2*a*, 5, 10). Most of them send a single



Figures 3-9. For description see opposite.

transverse process crossing the nerve cord midline or the central plexus adjacent to the cell body (figure 11).

The second type consisted of a large neuron with a cell body size (diameter *ca.*  $>25\ \mu\text{m}$ ) that corresponded to those of the giant neurons described by Cobb & Stubbs (1981). The cell body of the giant neuron was always located in the ganglion close to one central plexus and adjacent to the small monopolar neurons (GN; figures 2*a*, 10). There was generally one cell body per ganglion on one side of the nerve cord midline (figures 10, 14). Very often, a particular pattern consisting of single cell bodies alternating with each other on either side of the nerve cord midline was seen for a distance of 3–5 segments (figure 14). On a few occasions, a ganglion containing two cell bodies on opposite sides of the nerve cord midline was also observed (figure 12). All positive giant neurons were characterized by three processes, one transverse, ran across the nerve cord midline to the opposite central plexus, and two longitudinal ran in opposite directions on the same side as the cell body (figures 12, 13). The two longitudinal processes could be traced to the next ganglion where they became mixed with the other fibres of the central plexus (figure 14). It could not be ascertained whether each longitudinal process terminated in the next segment or continued for a longer distance. The transverse process could only be traced over the distance separating the central plexuses in the same ganglion (figure 12). As for the longitudinal processes, it could not be seen whether the transverse process ended in the opposite central plexus or divided into one or two branches running to the next ganglion.

(ii) *The proximal segments of the nerve cord and the ring*

The second proximal segment, like the more distal, contained at the periphery the four groups of immunoreactive cell bodies, and centrally, a single giant neuron and a large population of small monopolar neurons (figures 15*a*, 16, 17). However, a comparison with the more distal segments (compare figures 5 and 16) showed that in the second proximal

segment there were more positive cell bodies in the interganglion and more small monopolar neurons between the central plexuses.

In the first proximal segment, labelling was only observed between the central plexuses and consisted of 20–30 Y-shaped neurons (cell body diameter *ca.*  $15\ \mu\text{m}$ ) (figures 15*a*, 16, 18). Neither the giant neuron nor the peripheral neurons were detected in that segment (in the last case, probably because of the damage caused by the extraction of the segment from the skeletal plates). Immunoreactivity in the ring did not show the complicated pattern of distribution present in the nerve cord. However, here too, most of the labelling was concentrated in the ectoneural tissue and consisted of nerve plexuses running centrally and along the inner and outer edge of the ring (figure 20). The central and outer plexuses were in continuity with the central and the peripheral plexuses, respectively, of the nerve cord. The inner plexus was in continuity with that running in the adjacent ring branch. Two significant concentrations of positive monopolar neurons (cell body diameter *ca.*  $15\ \mu\text{m}$ ) were detected in each ring branch: one, proximally, along the inner edge, at the junction between two ring branches (figures 15*a*, 16, 19) and the other, more distally, along the outer edge (figures 15*a*, 20).

The hyponeural system, as in the radial nerve cord, was only weakly labelled. A few positive cell bodies and fibres were detected above the ectoneural cell bodies of the outer edge of the ring (figures 15*a*, 20).

In control experiments, preabsorption of S1 antiserum with S1 or KYSALMFamide mostly abolished the staining. However, a few weakly-positive cell bodies and fibres from both nerve cord and ring were still detected. This may imply another peptide related to S1 is present with some modest cross-reactivity and this should be borne in mind as further understanding of echinoderm neuropeptides is achieved. BL IIIb preabsorbed with RFamide did not block immunoreactivity, indicating that the antiserum does not cross-react with RFamide.

Figures 3–9. S1-Li IR in the radial nerve cord of *Ophiura ophiura*. Figure 3 is sectioned material, the rest are whole mounts.

Figure 3. Transverse section in a ganglion. The immunolabelling is located in the ectoneural tissue (E). There is no labelling in the hyponeural tissue (H). (Magn.  $\times 140$ .)

Figure 4. Immunoreactive axons in a hyponeural motor nerve (arrow). (Magn.  $\times 240$ .)

Figure 5. General view of the immunoreactivity in the ectoneural tissue showing the peripheral (PP), central (CP), and median (MP) plexuses and their associated cell bodies, PN<sub>3</sub>, PN<sub>4</sub>, GN, and CN. (PN<sub>1</sub> and PN<sub>2</sub> are not visible here). Note that the fibres are more densely packed in the ganglion (G) than in the interganglion (I). (Magn.  $\times 160$ .)

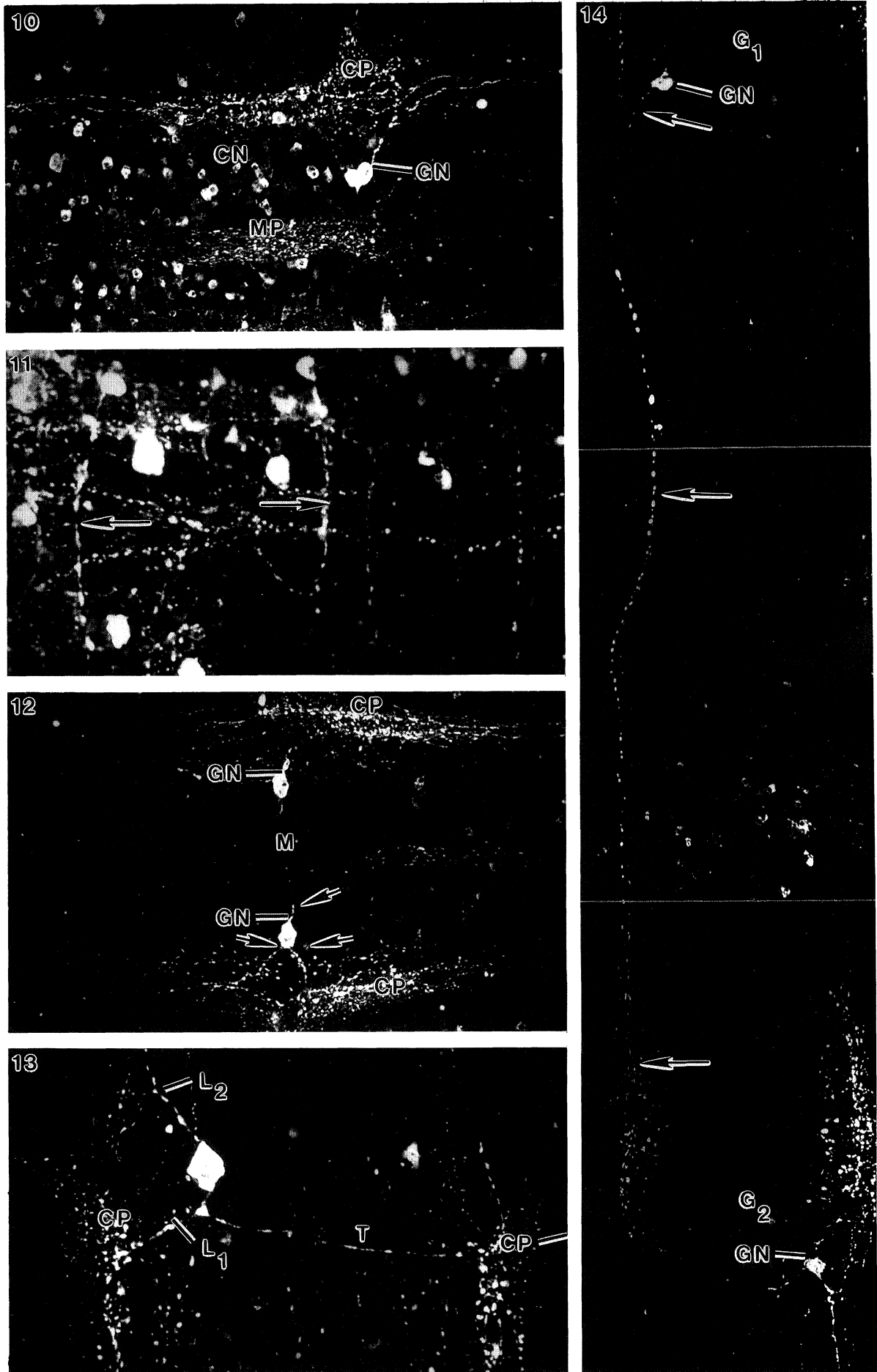
Figures 6–9. Immunoreactive cell bodies associated to the peripheral plexuses.

Figure 6. PN<sub>1</sub> beside the lateral branch (LB). Note the densely packed fibres running along the edge of the nerve cord and in the lateral branch. (Magn.  $\times 170$ .)

Figure 7. PN<sub>2</sub> at the base of the lateral branch (LB). Part of the central plexus (CP) is also shown. (Magn.  $\times 240$ .)

Figure 8. PN<sub>3</sub> between the peripheral plexus (PP) and the central plexus (CP). (Magn.  $\times 200$ .)

Figure 9. PN<sub>4</sub> in the interganglion (I). Part of the ganglion (G) and fibres of the central (CP) and median (MP) plexuses are also shown. (Magn.  $\times 70$ .)



Figures 10–14. For description see opposite.

**(b) RFamide-like immunoreactivity**

As with the S1 antiserum, the RFamide antiserum gave excellent labelling in whole mounts and made the comparison between the two distributions quite straightforward. The distribution pattern of RFamide-like immunoreactivity (RFa-Li IR) was very similar to that of S1. However, differences were clearly seen in the ectoneural tissue of both nerve cord and ring. The hyponeural tissue was weakly labelled by RFamide antiserum and no differences with S1 labelling could be detected.

**(i) The radial nerve cord**

The ectoneural tissue contained five strongly-positive plexuses and cell bodies whose distribution was identical in all segments of the nerve cord (figure 2*b*). Similarly to S1-Li IR, there were at the periphery of each ganglion three groups of positive cell bodies beside and at the base of the lateral branches, and between the peripheral and central plexuses (figure 2*b*). Between the central plexuses, there were 20–30 small monopolar neurons and a single giant neuron, the morphology and distribution of which were very similar to that seen with S1 labelling (figures 2*b*, 21). Although the RFamide-like distribution pattern was very similar to the S1-like, two distinct differences could be detected with the RFamide antiserum: (i) no positive cell bodies were detected at any time in the interganglia (figures 2*b*, 22); and (ii) the small monopolar neurons between the central plexuses were less numerous and were not immediately adjacent to the giant neuron (compare figures 2*a* and 2*b*; figures 5 and 21).

**(ii) The proximal segments of the nerve cord and the ring**

Both proximal segments are characterized by a large population of strongly immunoreactive monopolar neurons covering most of the width of the segments, except the periphery (figures 15*b*, 23). The ganglion of the second proximal segment contains the three groups of peripheral cell bodies as well as a single giant neuron (figure 15*b*).

In the first proximal segment, neither the giant neuron nor the peripheral cell bodies were observed (in this last case, probably because of the damage provoked by the dissection of the segment from the calcite plates). A comparison between RFamide-like and S1-like labelling (compare figures 15*a* and *b*,

figures 16 and 23) clearly showed that: (i) there were no RFamide positive neurons in the interganglion between the second and the first proximal segment; and (ii) both segments contained far more monopolar neurons in the RFamide-like distribution.

In the ring, the RFamide antiserum labelled nerve plexuses and cell bodies which were arranged similarly to S1-like distribution (figures 15*a* and *b*). A comparison of the cell body distribution between S1- and RFa-Li IR showed that: (i) at the junction nerve cord ring there were RFamide positive neurons extending in each ring branch (figures 5*b*, 23–25); and (ii) there was a larger population of RFa-like immunoreactive neurons along the ring outer edge (compare figures 20 and 26).

In control experiments, preabsorption of RFamide antiserum with RFamide totally abolished the staining in both nerve cord and ring. When RFamide antiserum was preabsorbed with KYSALMFamide or S1, no reduction of immunoreactivity was detected.

**4. DISCUSSION**

Immunocytochemistry on intact pieces of nerve cord and ring is very effective in the brittle star *Ophiura ophiura*. This approach is important because first, it generates reliable data concerning the organization of the nervous system, and second, it has demonstrated the localization and identification of a particular giant neuron with morphological characteristics similar to one class described from intracellular dye-fills (Cobb & Ghyoot 1993). In addition, by comparing the distribution obtained with SALMF- and RFamide antisera, the method gives an important clue to the possible presence of two distinct neuropeptides in the brittle star nervous system.

**(a) Organization of the nervous system in the brittle star**

Both antisera show an abundant immunoreactivity in the nerve cord and ring, providing good evidence that S1- and RFamide-like peptides have an important function in the brittle star nervous system. Immunolabelling is mostly observed in the ectoneural tissue and reveals a regional concentration of fibres and cell bodies, especially in the radial nerve cord. Two distinct regions can be seen: a central region

---

Figures 10–14. S1-Li IR in a ganglion of the radial nerve cord of *Ophiura ophiura*: the central plexuses and their associated cell bodies. All illustrations are whole mounts.

Figure 10. The giant neuron (GN) and beside it, the small monopolar neurons (CN). The central (CP) and median (MP) plexuses are shown. (Magn.  $\times 200$ .)

Figure 11. Small monopolar neurons sending transverse processes (arrows). (Magn.  $\times 440$ .)

Figure 12. Two giant neurons (GN) in the same ganglion on opposite sides of the nerve cord midline (M). The lower neuron clearly has three processes (arrows). (Magn.  $\times 200$ .)

Figure 13. Giant neuron (GN) with its three processes: two longitudinal ( $L_1$ ,  $L_2$ ) joining the central plexus (CP) on the same side as the cell body, and one transverse (T) joining the opposite central plexus (CP'). (Magn.  $\times 300$ .)

Figure 14. General view of two successive ganglia ( $G_1$  and  $G_2$ ) showing two giant neurons (GN) alternating on each side of the nerve cord. One of the longitudinal process of the giant neuron from  $G_1$  (arrow) is running down to  $G_2$ . (Magn.  $\times 190$ .)



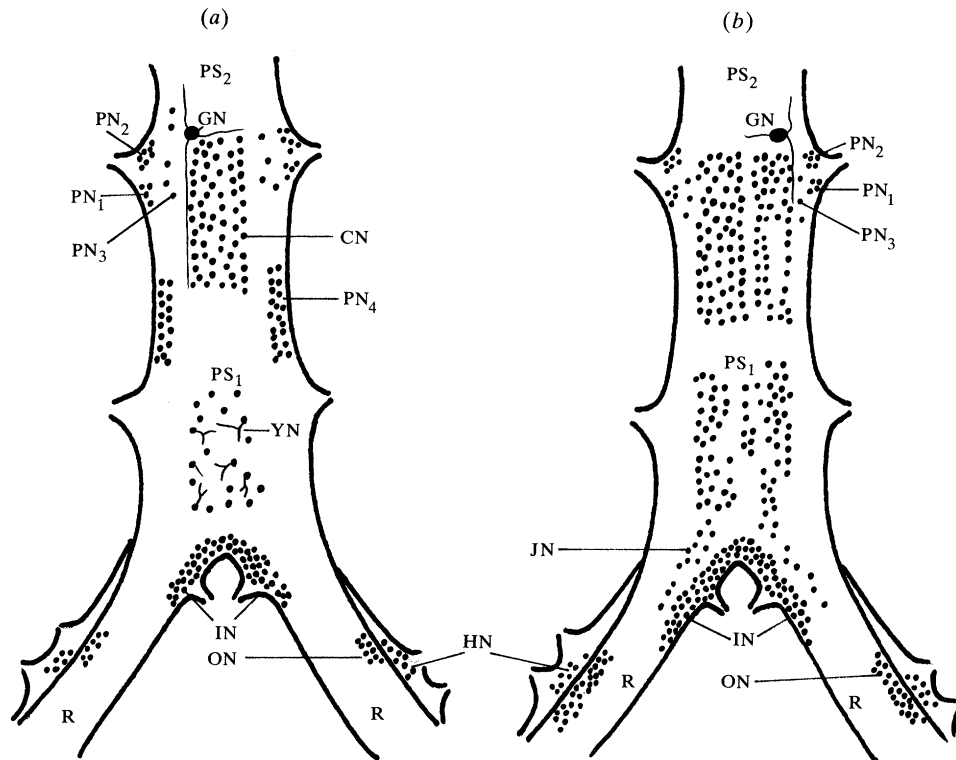


Figure 15. Schematic representation of the immunolabelling in the proximal segments of the radial nerve cord and the ring of *Ophiura ophiura* (the fibre plexuses are not represented): (a) S1-Li IR; (b) RFa-Li IR. In S1-Li IR, the second proximal segment (PS<sub>2</sub>), like the more distal segments, contains the four groups of peripheral neurons (PN<sub>1</sub>, PN<sub>2</sub>, PN<sub>3</sub>, PN<sub>4</sub>), and between the central plexuses a single giant neuron (GN) and the population of small monopolar neurons (CN). The first proximal segment (PS<sub>1</sub>) only contains a small group of Y-shaped neurons situated centrally (YN). In the ring, immunoreactive ectoneural cell bodies are distributed along the inner and outer edges of each branch (IN and ON, respectively). Positive hyponeural cell bodies (HN) are located on the outside of the outer edge neurons.

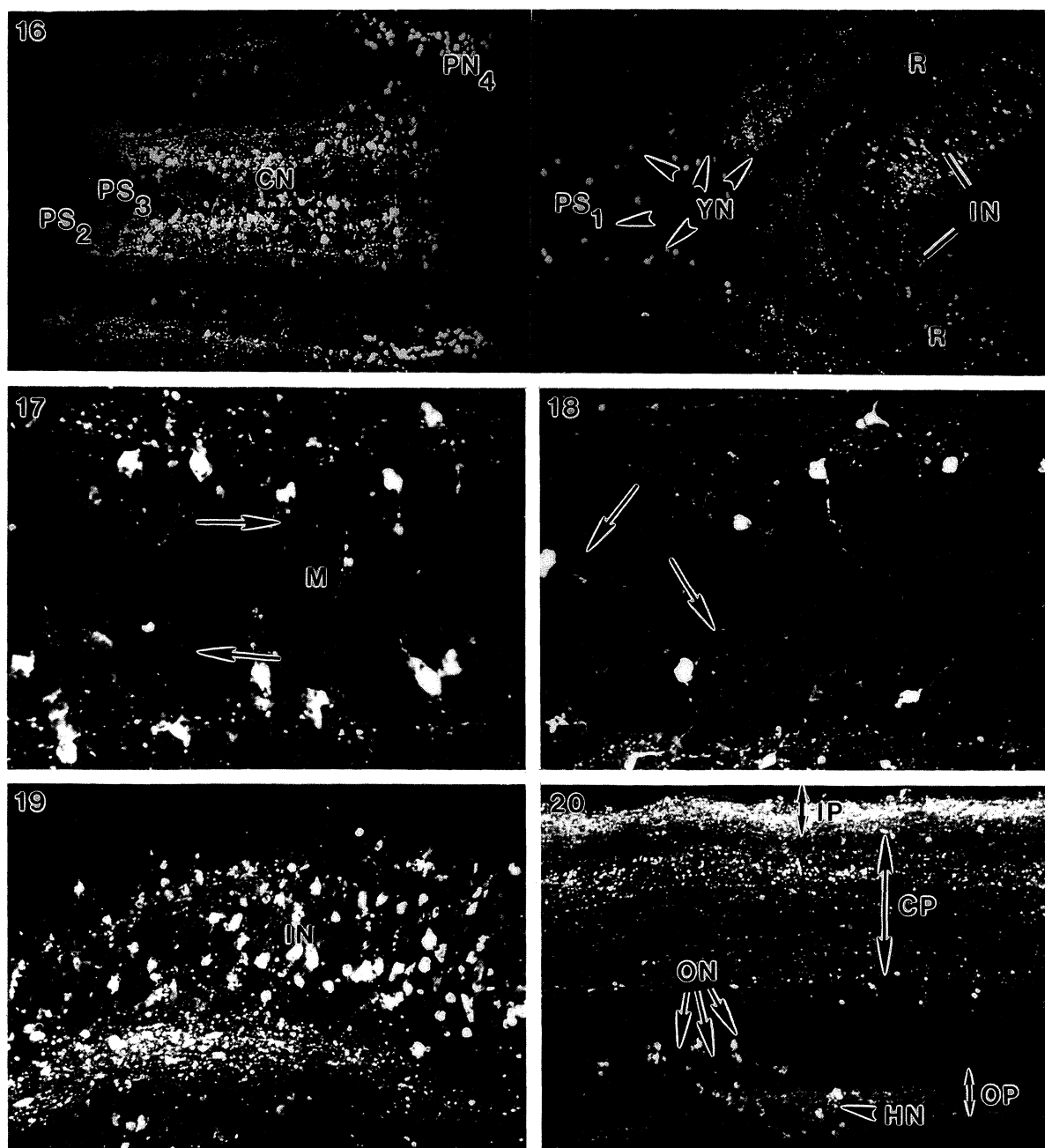
Comparison between (a) and (b) shows that in RFamide-like distribution: (i) there are no peripheral neurons (PN<sub>4</sub>) in the interganglion between the second and the first proximal segments; (ii) both segments contain far more neurons; (iii) a group of scattered neurons (JN) are detected from the junction nerve cord-ring to the proximal portion of each ring branch; and (iv) there are more labelled cell bodies along the outer edge of the ring (ON).

occupying most of the width of the nervous tissue and a peripheral one restricted to the lateral edges. Similar features were observed with GABA antiserum (Ghyoot & Cobb 1994). The significance of these distinct regions is far from clear. A possible interpretation is that the central neurons are largely involved in rapid through conducting of information about whole animal behaviour and that the peripheral neurons co-ordinate local responses, such as tubefeet movements over more local regions of a few segments. This division into central and peripheral pathways has not been obvious using other techniques and clearly requires further study.

Immunostaining with both antisera reveals particular anatomical features in the ectoneural system of the radial nerve cord and the ring. In the radial nerve cord, both antisera demonstrate that it is segmentally organized. That is, the pattern of immunoreactivity observed in one segment is identical to that of the adjacent. The segmental organization of the nerve cord was previously reported by Cobb & Stubbs (1981) but only for the giant neurons. This idea is

extended in the present study and indicates a repetitive organization for all the neurons of the nerve cord. This segmental organization is not only revealed by S1 and RFamide antisera. Investigations using antisera against GABA, glycine and 5-HT also lead to similar conclusions (Ghyoot & Cobb 1994). Such studies highlight the value of employing panels of antisera raised against a range of transmitters to demonstrate the complexity of neuronal networks.

Contrary to statements in the literature (Cobb & Stubbs 1981, 1982), the second and first proximal segments of the nerve cord are anatomically distinct from the more distal segments and must therefore represent a specialized region. Indeed, both antisera show that the second proximal segment contains more immunoreactive neurons and that the first one displays a distribution pattern different from the other segments. These segments, however, show no real difference in size and as they are involved with innervating various features of the disc as well as providing connections in both directions round the



Figures 16–20. S1-Li IR in the proximal segments of the radial nerve cord and the ring in *Ophiura ophiura*. All illustrations are whole mounts.

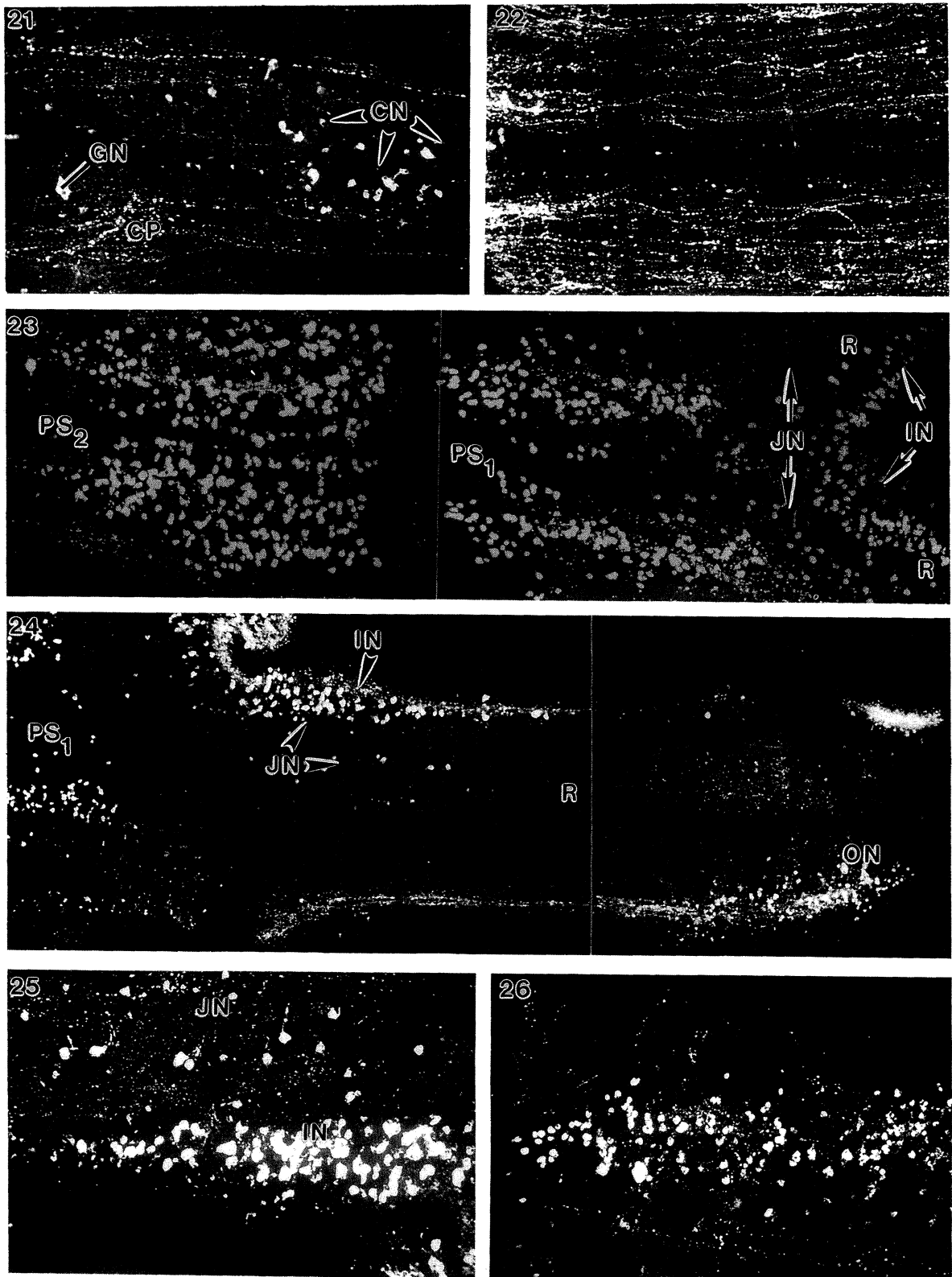
Figure 16. General view of the immunolabelling in the proximal segments and part of the ring. The second proximal segment (PS<sub>2</sub>) is characterized by a large population of small central monopolar neurons (CN) and an important group of peripheral neurons (PN<sub>4</sub>) in the interganglion. The first proximal segment (PS<sub>1</sub>) only contains a small group of Y-shaped neurons (YN). The inner edge of each ring branch (R) shows an important concentration of immunoreactive cell bodies (IN). (Magn. × 80.)

Figure 17. Central neurons of the second proximal segment sending monopolar processes (arrows) towards the nerve cord midline (M). (Magn. × 300.)

Figure 18. Y-shaped neurons (arrows) of the first proximal segment. (Magn. × 220.)

Figure 19. Immunoreactive neurons (IN) along the inner edge of a ring branch. (Magn. × 180.)

Figure 20. General view of the distal part of a ring branch. There are fibre plexuses running along the inner and outer edges (IP and OP, respectively) and centrally (CP). Ectoneural and hyponeural cell bodies (ON and HN, respectively) are detected along the outer edge of the ring branch. (Magn. × 100.)



Figures 21–26. For description see opposite.

ring to adjacent radii, a different layout is to be expected. These segments cannot have the complex integrative function suggested by Smith (1966). It is likely they are, however, associated with such essential disc functions as mouth movements, control of gonad development and release of gametes.

In the ring, immunoreactivity is simple and contrasts markedly with more complex patterns seen in the radial nerve cord. Regional concentrations of cell bodies along the inner and outer edges of the ring are likely to be involved as local ganglia controlling organs innervated by the ring branches. Staining mainly consists of fibres which are continuous with those running in the nerve cord. This study thus confirms previous ultrastructural results (Cobb & Stubbs 1982) that the ring cannot be regarded as a central nervous system but only functions as a link between the five segmented nerve cords.

Although immunoreactivity is very weak in the hyponeural tissue, positive staining here may suggest that this tissue is not simply composed, as previously thought, of a single population of cholinergic motor neurons (Stubbs & Cobb 1981). These results combined with the positive staining obtained with GABA antiserum (Ghyoot & Cobb 1994) may indicate that the organization of the hyponeural tissue in brittle star nervous system is more complex. It must be remembered, however, that no labelled cell bodies were detected anywhere in the hyponeural tissue of the radial nerve cord. There is therefore the possibility that the stained fibres are ectoneural. Although it has been assumed that there are no direct connections between the ectoneural and the hyponeural nervous systems, there is a published account of small fibre tracts from the ectoneural passing through gaps in the separating basement membrane into the hyponeural nervous system (Stubbs & Cobb 1981). These are present in every segment in the same position and may represent branches of interneuronal or sensory nerves penetrating into the deep tissue of the arm. As proprioceptors are known to exist from physiological evidence but have not been anatomically described, maybe the labelled axons are nerve tracts from them. At present this seems a likely explanation for the apparent staining of hyponeural nerves.

### (b) Identification of a giant neuron

Each ganglion of the nerve cord contains one, or occasionally two, immunoreactive giant neurons characterized by three processes: two longitudinal running in opposite directions on the same side as the cell body, and one transverse running across the nerve cord midline to the opposite central plexus. Although it was not possible to trace the transverse process for any longer distance, the shape of this neuron is reminiscent of that of the H-cell which has been identified by dye-filling with carboxyfluorescein (Cobb & Ghyoot 1993). The H-cell, like the immunoreactive giant neuron, has three processes: two longitudinal and one transverse, ramifying on the other side of the nerve cord midline into two branches parallel to the longitudinal processes. Dye-filling also shows that each longitudinal process runs for 2–4 segments without making synaptic connections within that distance. Although the function of the H-cell has not been characterized, it is readily impaled. What is not clear is whether there is one H-shaped cell in each segment (which is labelled by SALMF- and RFamide antisera) or whether there is a modest population perhaps containing other neuromodulators. Most of the giant neuron types described (See Cobb & Ghyoot 1993) pass through several segments without apparently making synaptic output or receiving input, and the significance of this has yet to be established. The real importance of this is that the immunoreactive giant neuron may well be individually identifiable and allow it to be used for repeatable intracellular studies.

### (c) Indication of two distinct neuropeptides

The pattern of S1-Li IR is very similar to that obtained with RFamide antiserum. However, since preabsorption indicates no cross-reactivity between antisera, it seems likely that the antisera are labelling different molecules. Where the pattern of immunoreactivity is co-incident, there is the strong possibility that the two peptides co-exist. This will need to be tested using serial sections and primary antisera raised in different species. Evidence that two distinct neuropeptides do exist in the brittle star is also confirmed by the fact that some neurons react to only one antiserum. Indeed, there are, in the interganglia

Figures 21–26. RFA-Li IR in the radial nerve cord and the ring of *Ophiura ophiura*. All illustrations from whole mounts.

Figure 21. Immunoreactivity in a ganglion of the radial nerve cord showing between the central plexuses (CP), a giant neuron (GN) and a small group of monopolar neurons (CN). (Magn.  $\times 140$ .)

Figure 22. Immunoreactivity in an interganglion of the radial nerve cord showing no labelled cell bodies at the periphery. (Magn.  $\times 140$ .)

Figure 23. General view of the immunoreactivity in the second (PS<sub>2</sub>) and first (PS<sub>1</sub>) proximal segments of the radial nerve cord and part of the ring (R). Both segments are characterized by a large population of immunoreactive neurons. At the junction nerve cord-ring, there are scattered neurons (JN) extending in each ring branch. An important concentration of positive cell bodies (IN) are detected along the inner edge of each ring branch. (Magn.  $\times 100$ .)

Figure 24. General view of the immunoreactivity in a ring branch showing the distribution of immunoreactive cell bodies: IN occurring proximally along the inner edge; ON located more distally along the outer edge; and JN situated below the inner edge neurons. (Magn.  $\times 80$ .)

Figure 25. Closer view of the inner edge of a ring branch showing the IN and JN neurons. (Magn.  $\times 130$ .)

Figure 26. Closer view of the ON neurons. (Magn.  $\times 130$ .)

of the radial nerve cord, a group of cell bodies only stained by the S1 antiserum, and in the proximal segments of the nerve cord and the ring, cell bodies only positive with the RFamide antiserum.

In this respect, it is difficult to speculate on the nature of S1- and RFamide-Li peptides. Five neuropeptides have been now isolated from echinoderm nervous systems: two asteroid peptides S1 and S2 in *A. rubens* and *A. forbesi* (Elphick *et al.* 1991a), one echinoid peptide with the amino acid sequence FPVGRVHRFamide in *Echinus esculentus* (Elphick *et al.* 1992) and two holothuroid peptides with the sequence GFSKLYFamide and SGYSVLYFamide in *Holothuria glaberrima* (Miranda *et al.* 1992). According to these last authors, four of the peptides define a novel family sharing the common C-terminal sequence SxLxF where 'x' can be occupied by any other residue. Although neuropeptides have not yet been isolated from brittle stars, it seems reasonable to predict that such molecules are present and will be members of the SxLxFamide family. The RFamide antiserum used here is unlikely to stain the peptides belonging to the new echinoderm family. First, the RFamide antiserum does not cross-react with S1, a member of that family; second, preabsorption controls of the antibody with RFamide abolish all staining. There are FaRPs that are probably FMRFamide homologues and there are FaRPs that are likely to be analogous. This is a difficult area, and Price & Greenberg (1989) have discussed this question in detail. The RFamide isolated from sea-urchin (FPVGRVHRFamide; Elphick *et al.* 1992) definitely falls into the analogue category, and it is a possibility that a molecule like this also exists in brittlestars and is responsible for the RFamide-like staining described in the current study. However, another possibility is that the RFamide antiserum is reacting with a brittlestar Neuropeptide-Y-like molecule. NPY-like peptides have been isolated from several invertebrate phyla and they all have a C-terminal RFamide sequence that would be recognized by the RFamide antiserum used in this study. Therefore, there is a strong possibility that this is the case, and this question should be addressed in future studies.

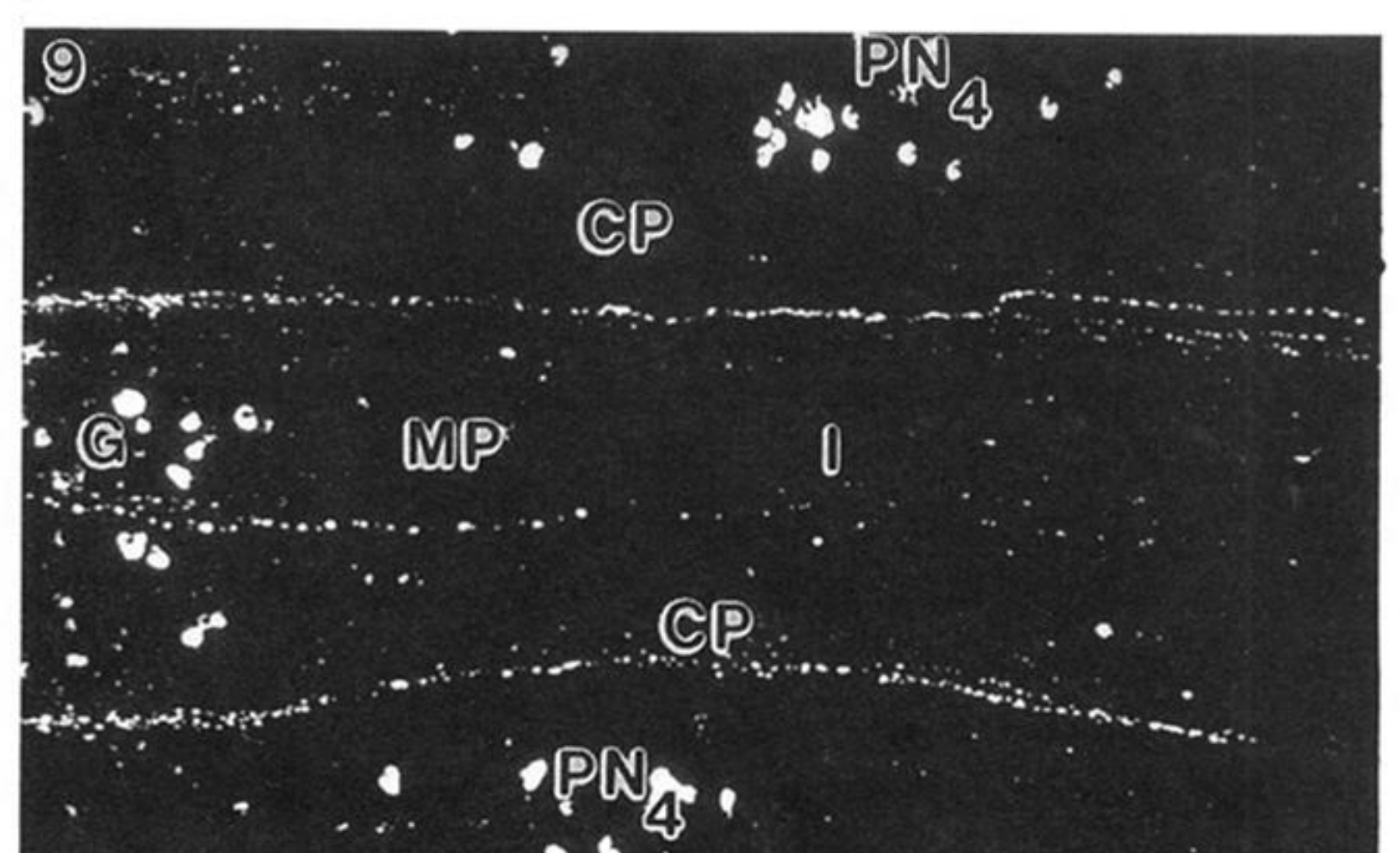
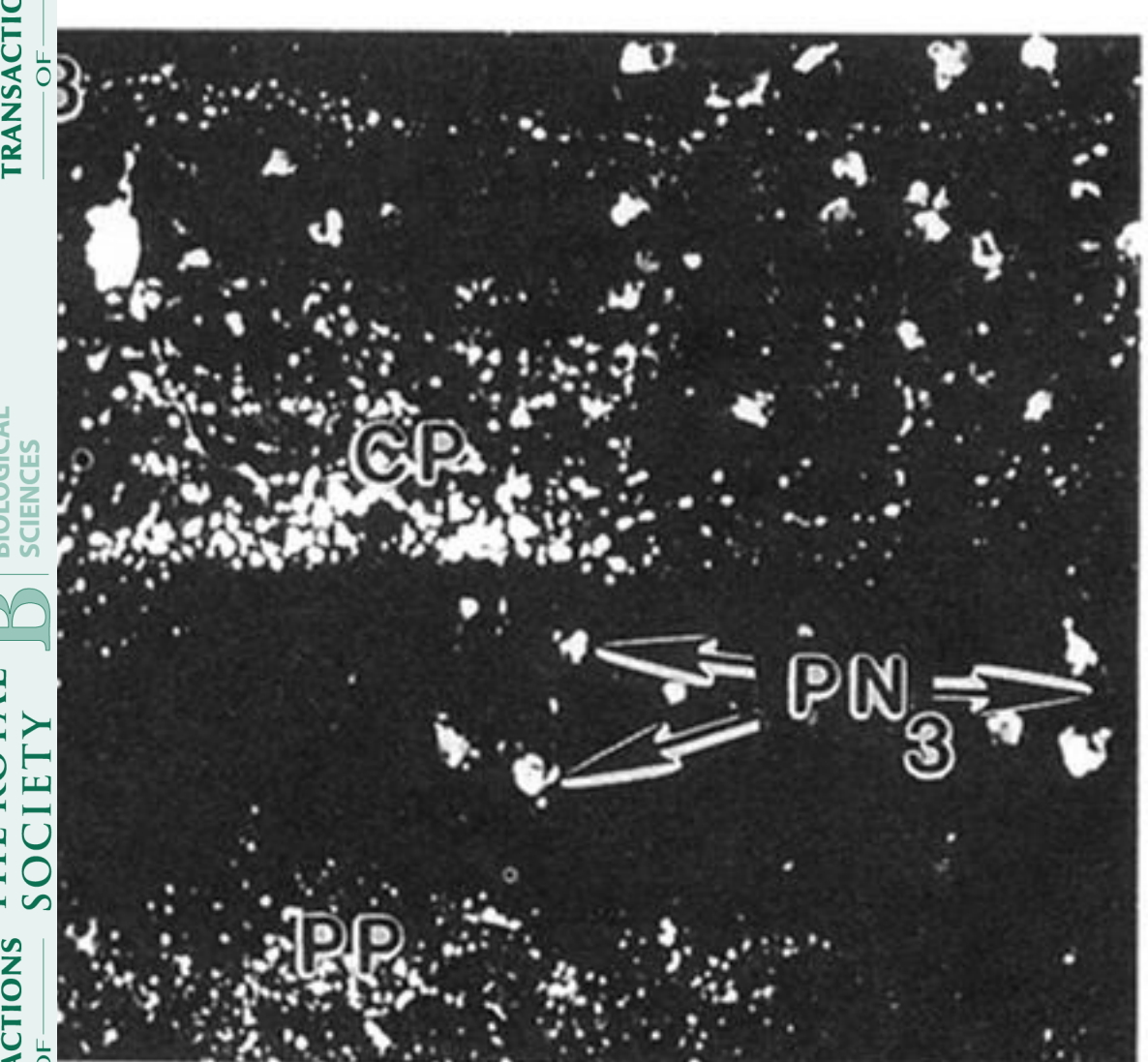
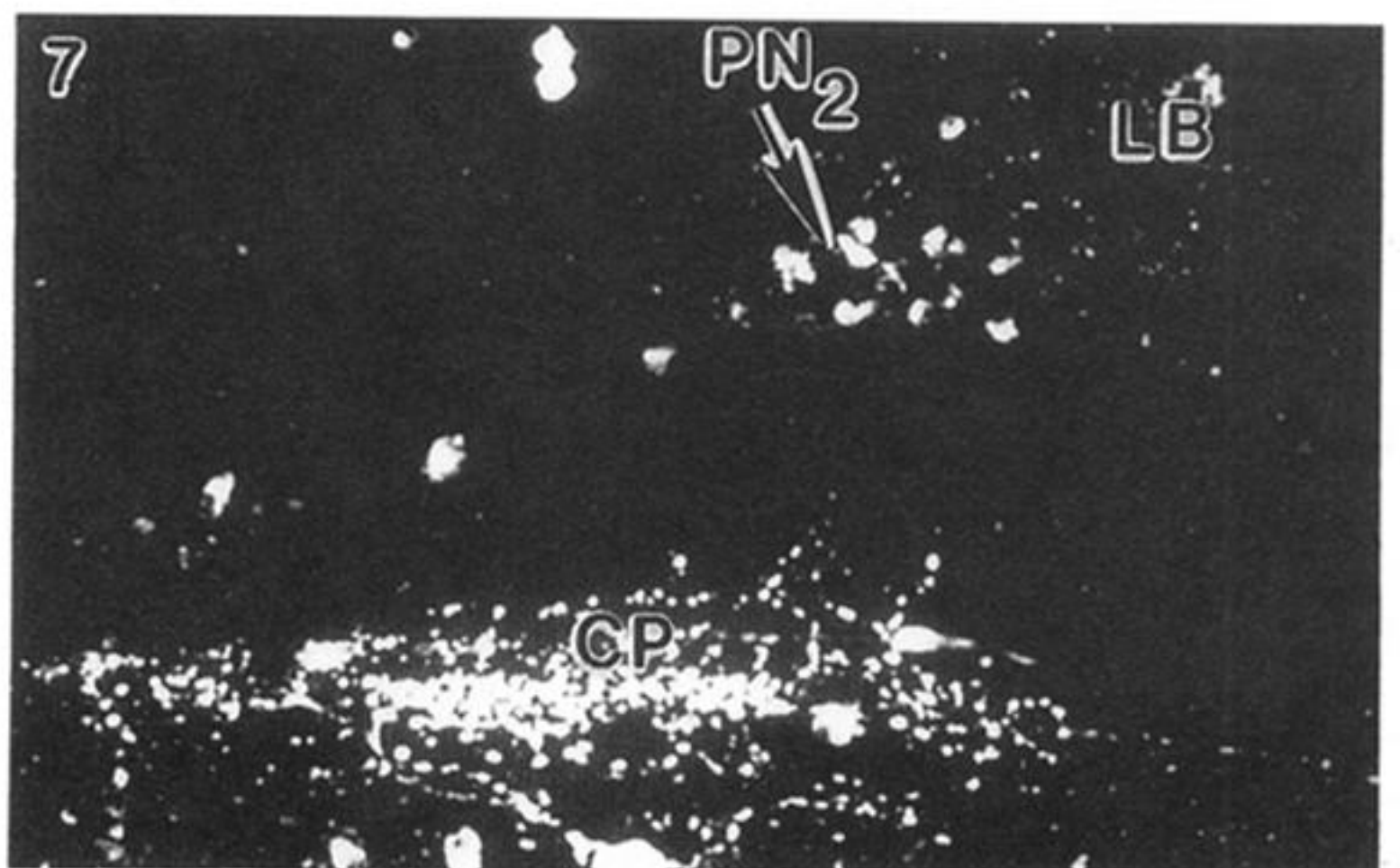
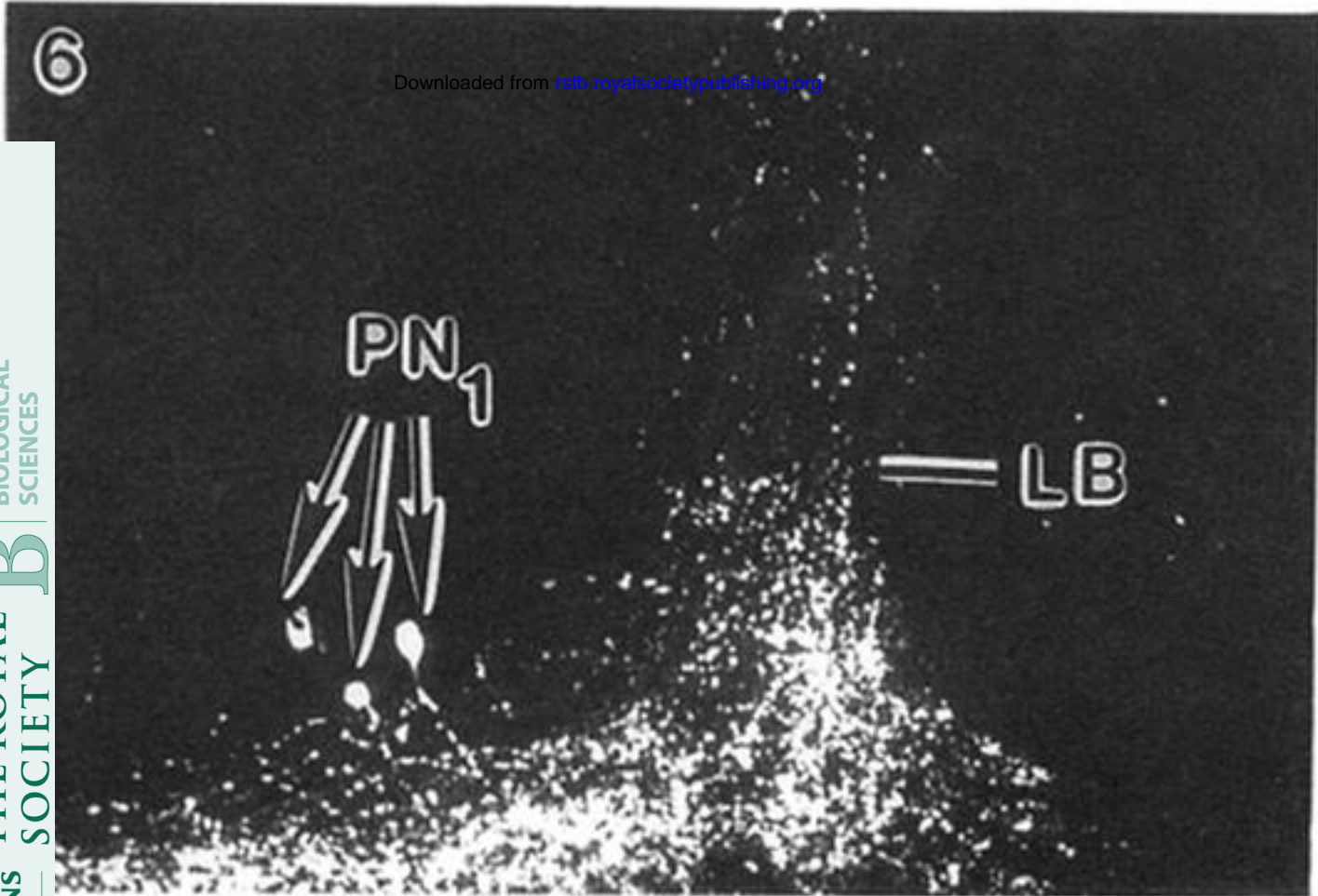
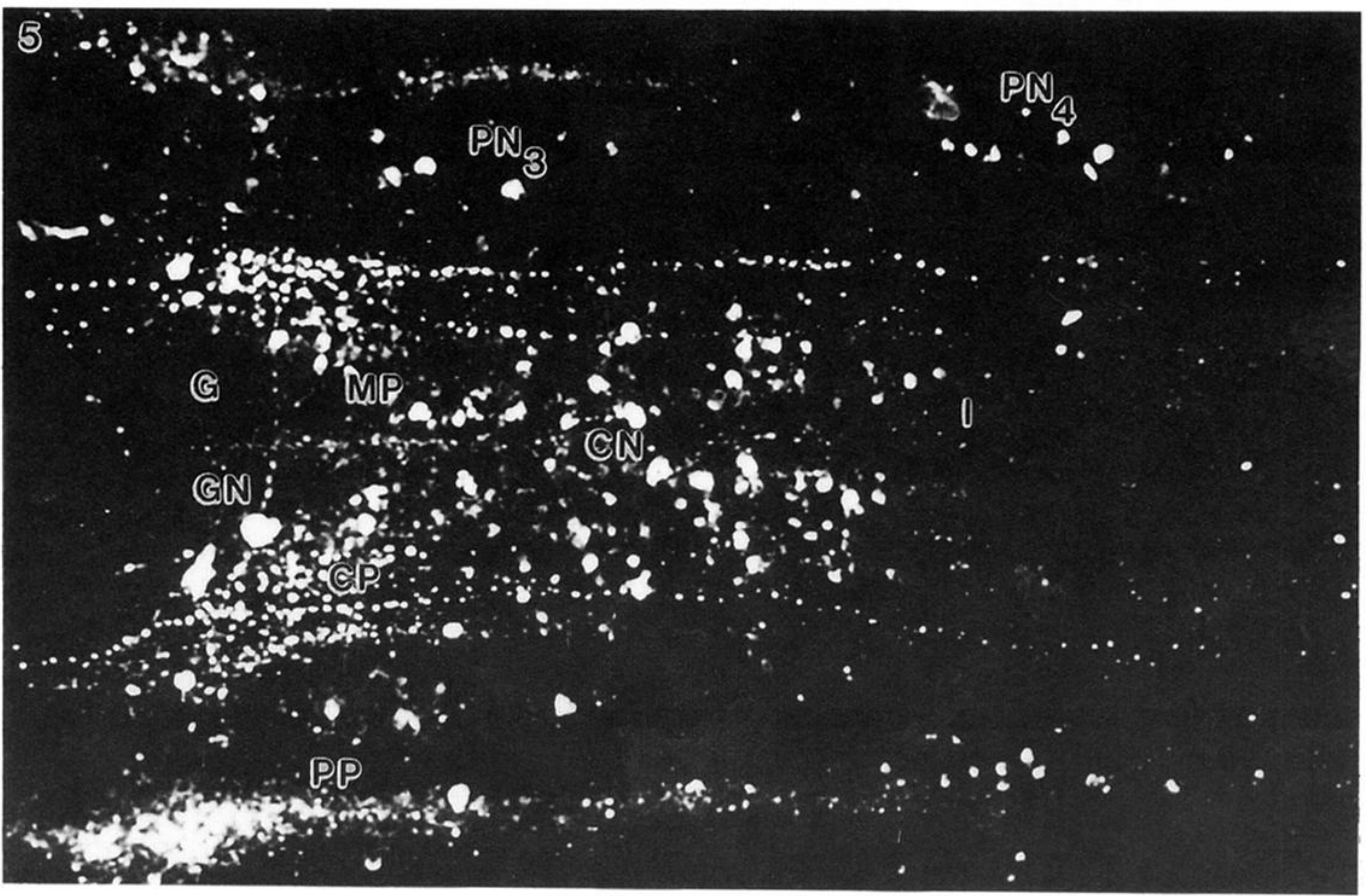
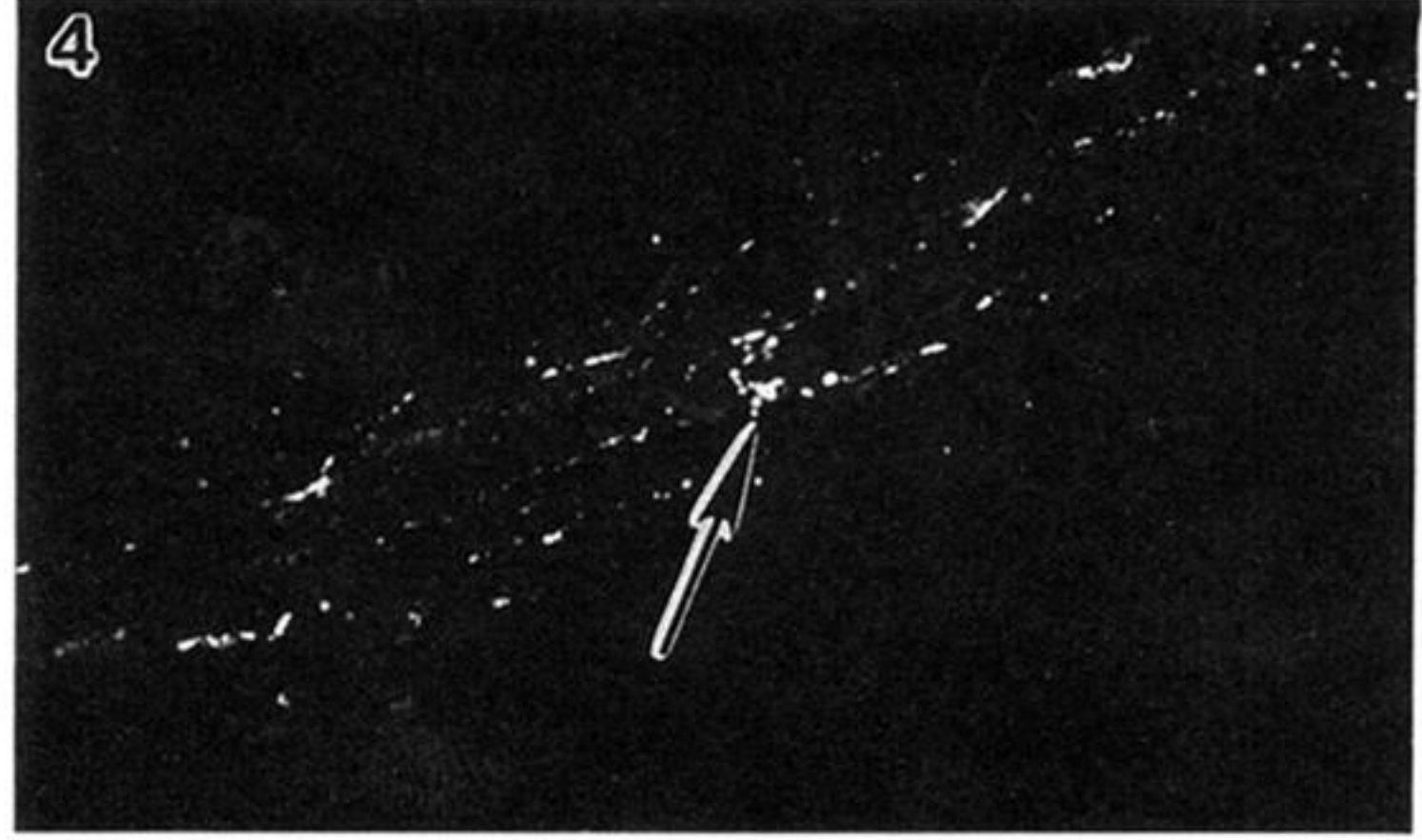
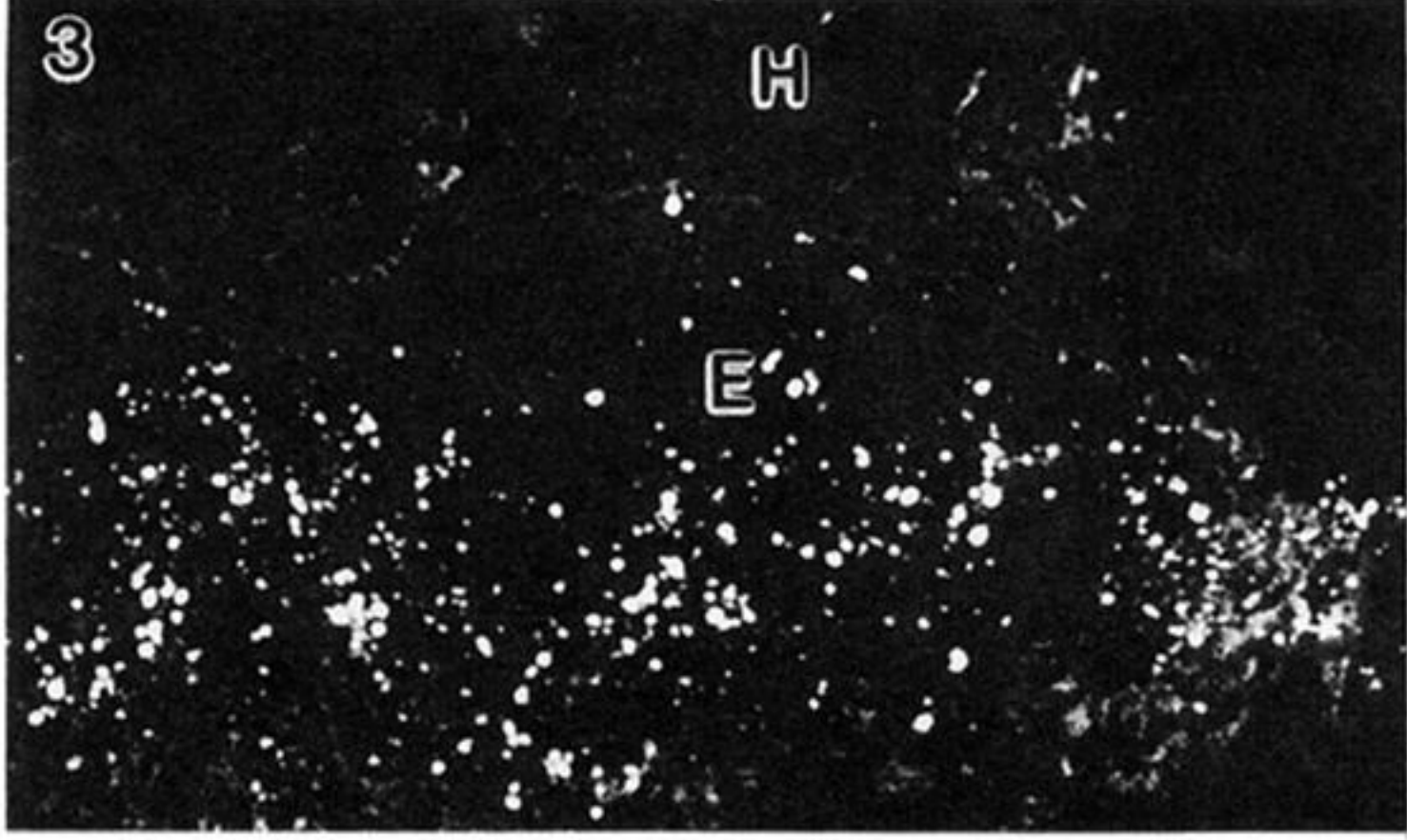
This work was supported by an EEC grant number SC1000346. We thank Professor Grimmelikhuijzen for the kind gift of the probe against RFamide.

## REFERENCES

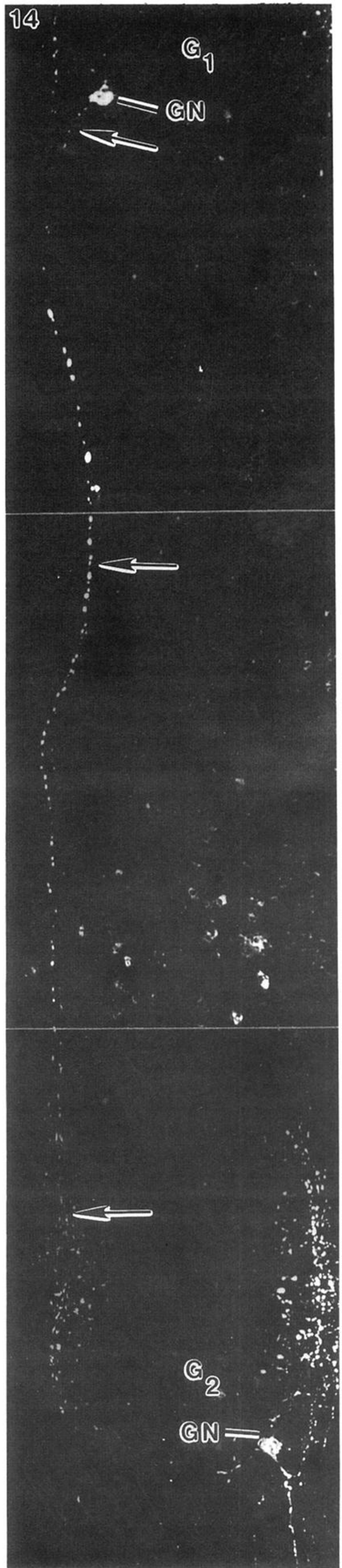
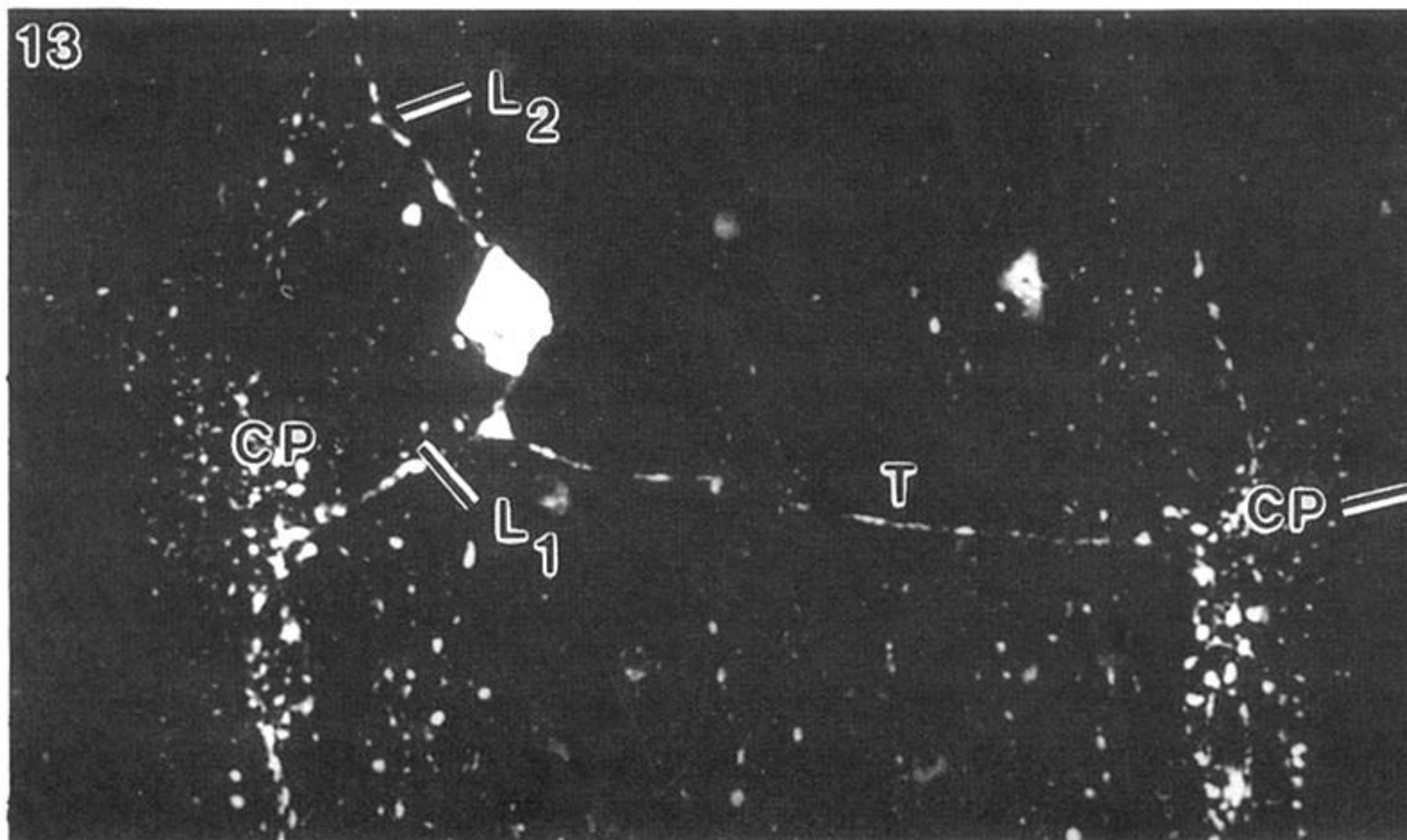
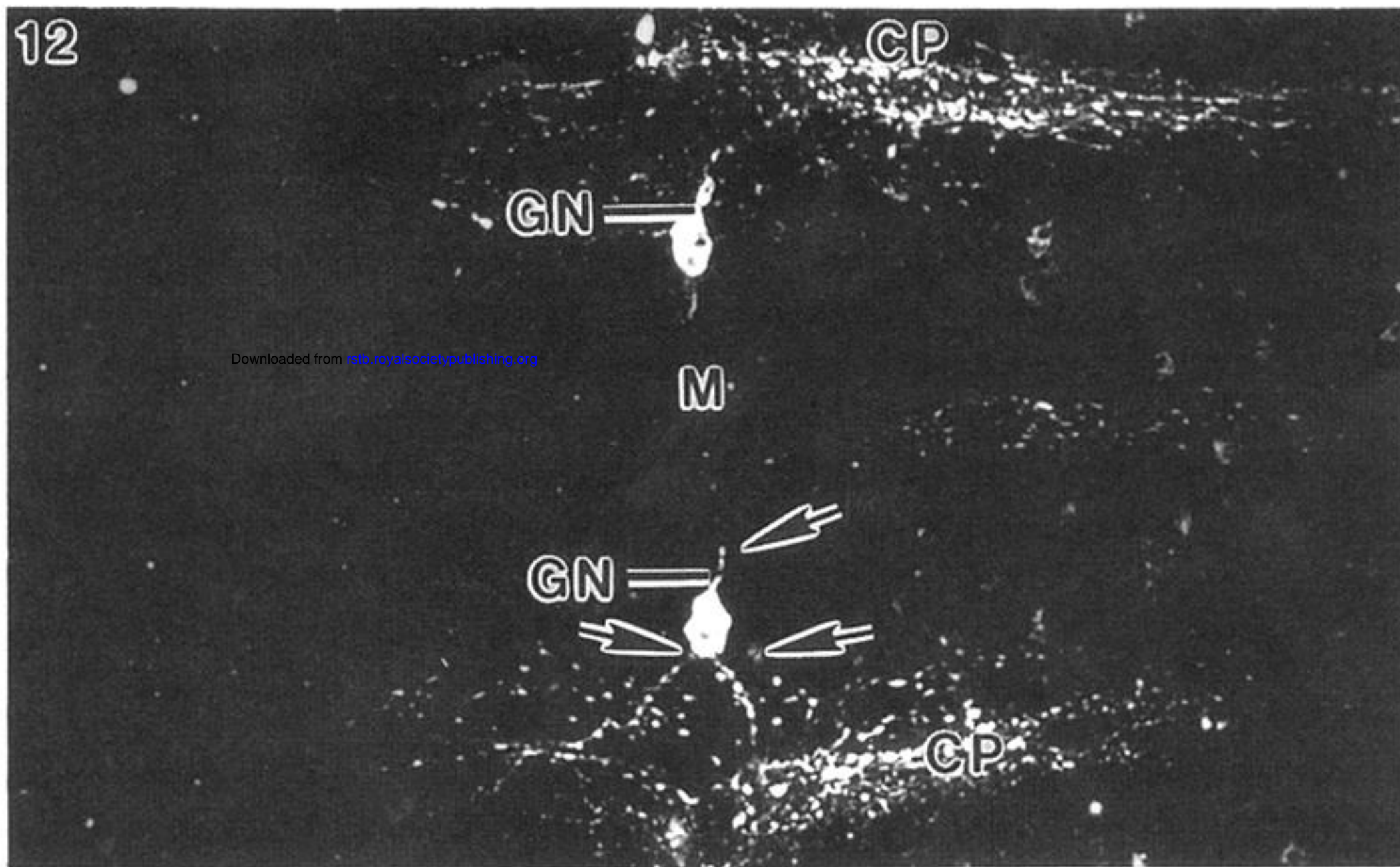
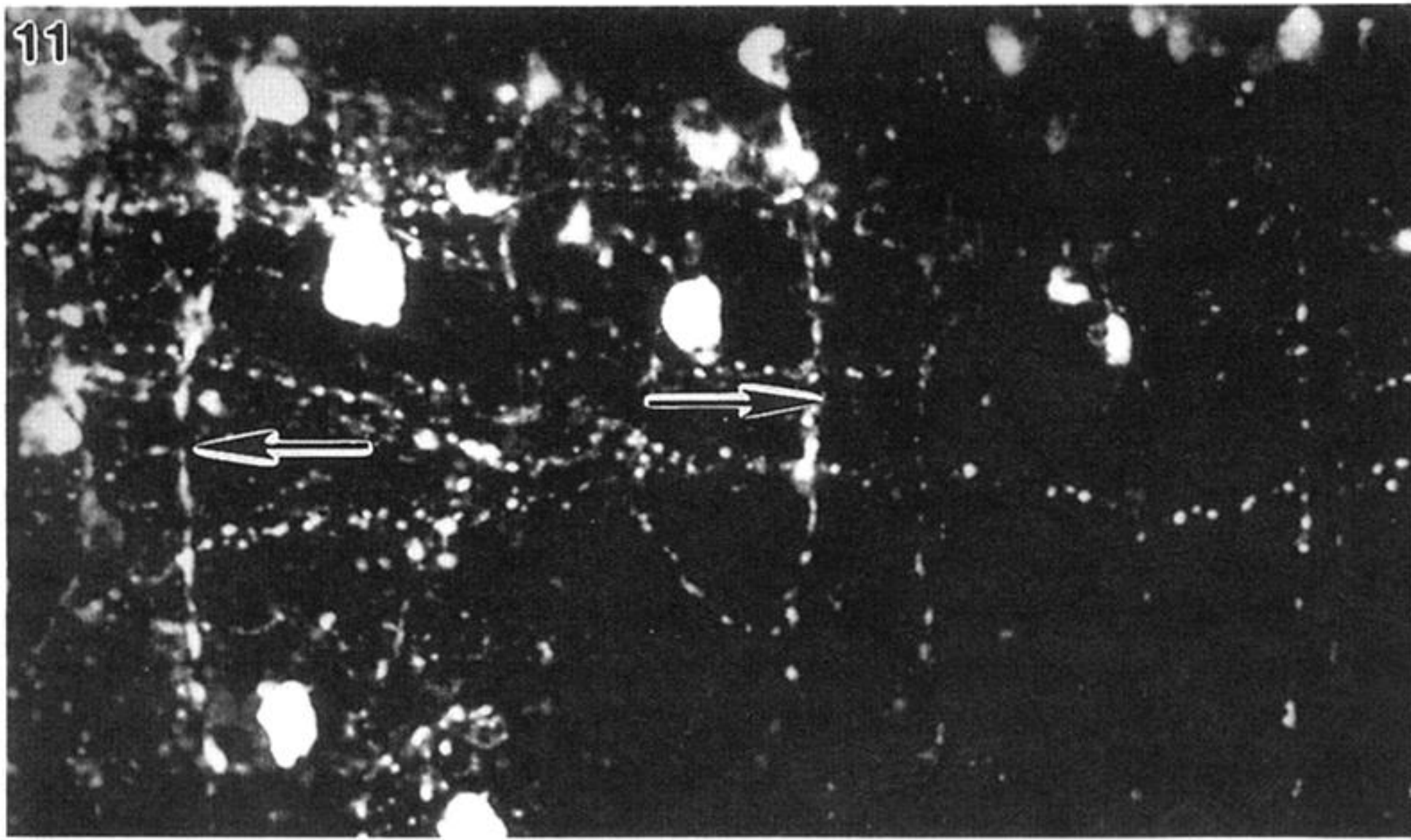
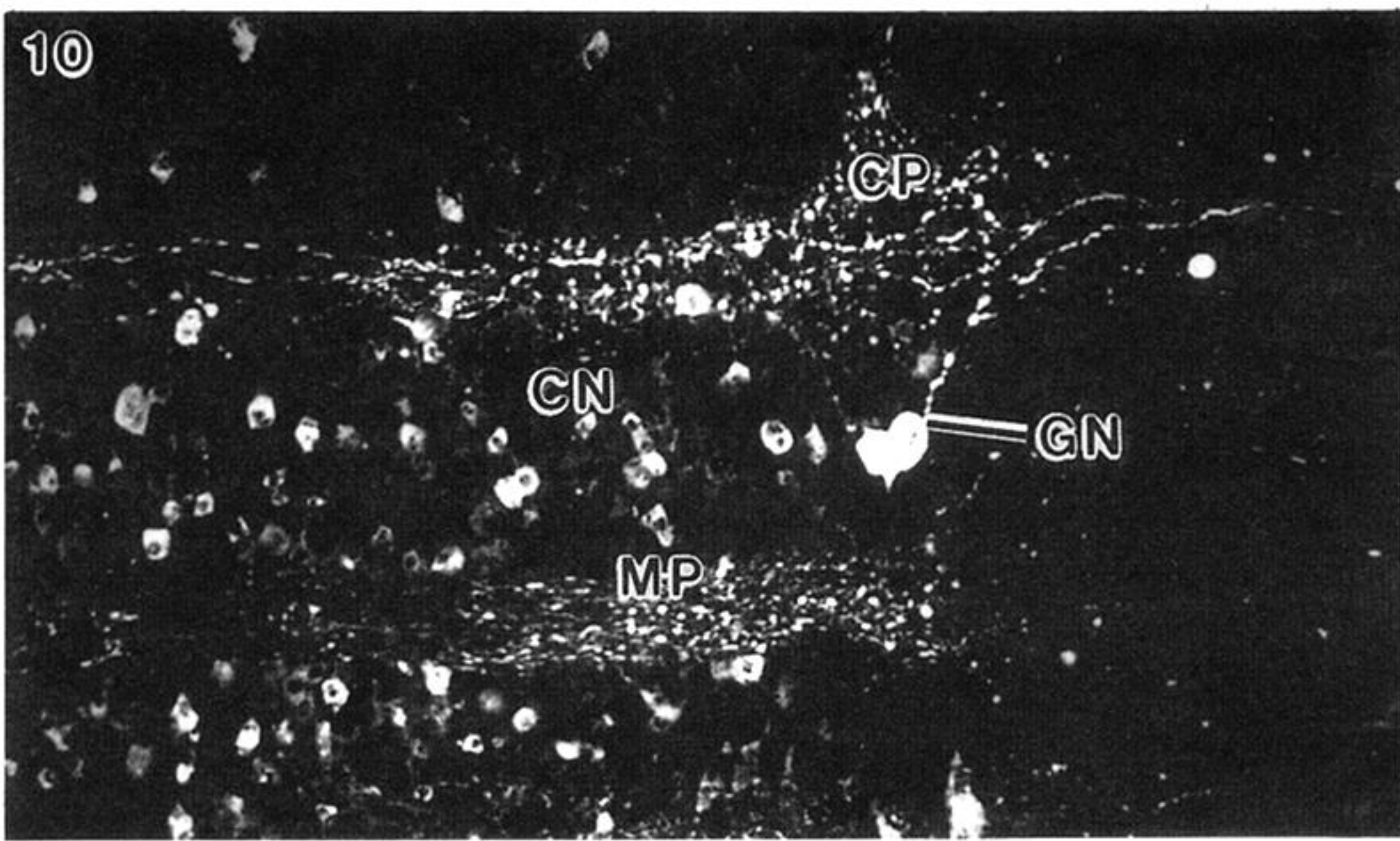
Cobb, J.L.S. 1985 The neurobiology of the ectoneural/hyponeural synaptic connection in an echinoderm. *Biol. Bull.* **168**, 432–446.

- Cobb, J.L.S. & Ghyoot, M. 1993 The giant through conducting neuron of the brittle star *Ophiura ophiura*. *Comp. Biochem. Physiol.* **105A**, 697–703.
- Cobb, J.L.S. & Stubbs, T.R. 1981 The giant neuron system in Ophiuroids. I. The general morphology of the radial nerve cords and the circumoral nerve ring. *Cell. Tissue Res.* **219**, 197–207.
- Cobb, J.L.S. & Stubbs, T.R. 1982 The giant neuron system in Ophiuroids. III. The detailed connections of the circumoral nerve ring. *Cell. Tissue Res.* **226**, 675–687.
- Diaz-Miranda, L., Price, D.A., Greenberg, M.J., Lee, T.D., Doble, K.E. & Garcia-Ararras, J.E. 1992 Characterization of two novel neuropeptides from the sea cucumber *Holothuria glaberrima*. *Biol. Bull.* **182**, 241–247.
- Elphick M.R. 1991 Neuropeptide structure and function in echinoderms. PhD Thesis University of London.
- Elphick, M.R., Emson, R.H. & Thorndyke, M.C. 1989 FMRFamide-like immunoreactivity in the nervous system of the starfish *Asterias rubens*. *Biol. Bull.* **177**, 141–145.
- Elphick, M.R., Parker, K. & Thorndyke, M.C. 1992 Neuropeptides in sea urchins. *Reg. Peptides* **39**, 265.
- Elphick, M.R., Price, D.A., Lee, T.D. & Thorndyke, M.C. 1991a The SALMFamides: a new family of neuropeptides isolated from an echinoderm. *Proc. R. Soc. Lond. B.* **243**, 121–127.
- Elphick, M.R., Reeve, J.R., Burke R.D. & Thorndyke, M.C. 1991b Isolation of the neuropeptide SALMFamide-1 from the starfish using a new antiserum. *Peptides* **12**, 455–459.
- Ghyoot, M. & Cobb, J.L.S. 1994 Immunocytochemical investigations on the radial nerve cord of *Ophiura ophiura*. Proceedings 8th International Echinoderm Conference, Dijon, 1993. (In the press.)
- Grimmelikhuijzen, C.J.P. 1985 Antisera to the sequence Arg-Phe-amide visualize neuronal centralization in hydroid polyps. *Cell. Tissue Res.* **241**, 171–182.
- Moore, S.J. & Thorndyke, M.C. 1993 Immunocytochemical mapping of the novel echinoderm neuropeptide SALMFamide 1 (S1) in the starfish *Asterias rubens*. *Cell Tiss Res.* **274**, 605–618.
- Price, D.A. & Greenberg, M.J. 1977 Structure of a molluscan cardioexcitatory neuropeptide. *Science* **197**, 670–671.
- Price, D.A. & Greenberg, M.J. 1989 The hunting of the FaRPs: The distribution of the FMRFamide-related peptides. *Biol. Bull.* **177**, 198–205.
- Smith, J.E. 1966 The form and functions of the nervous system. In *Physiology of the Echinodermata* (ed. R. A. Boolotian), pp. 503–512. New York: Interscience.
- Stubbs, T.R. & Cobb, J.L.S. 1981 The giant neuron system in Ophiuroids. II. The hyponeural motor tracts. *Cell. Tissue Res.* **220**, 373–385.
- Thorndyke, M.C., Crawford, B.D., Burke, R.D. 1992 Localization of a SALMFamide neuropeptide in the larval nervous system of the sand dollar, *Dendraster excentricus*. *Acta Zool.* **73**, 207–212.

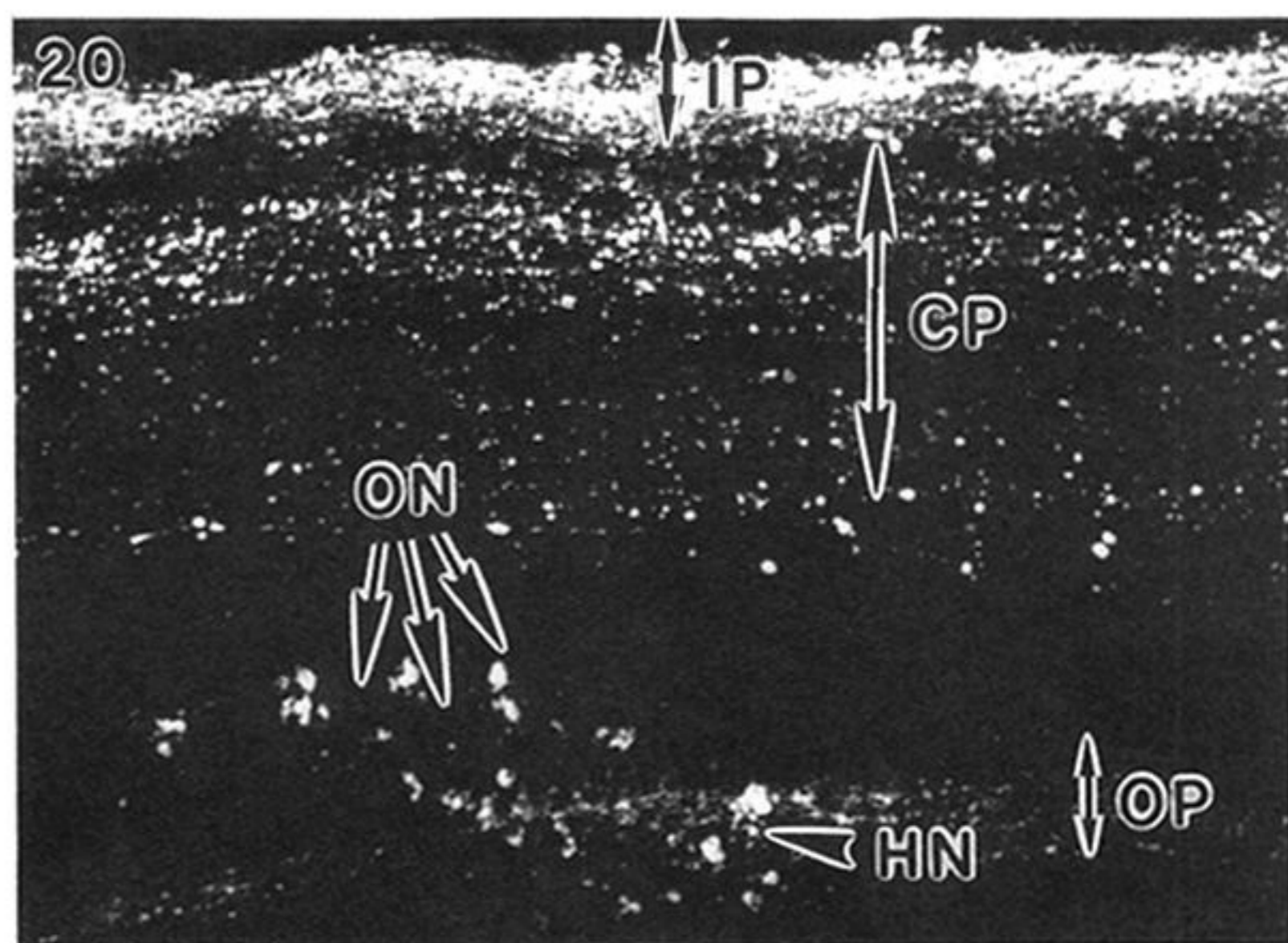
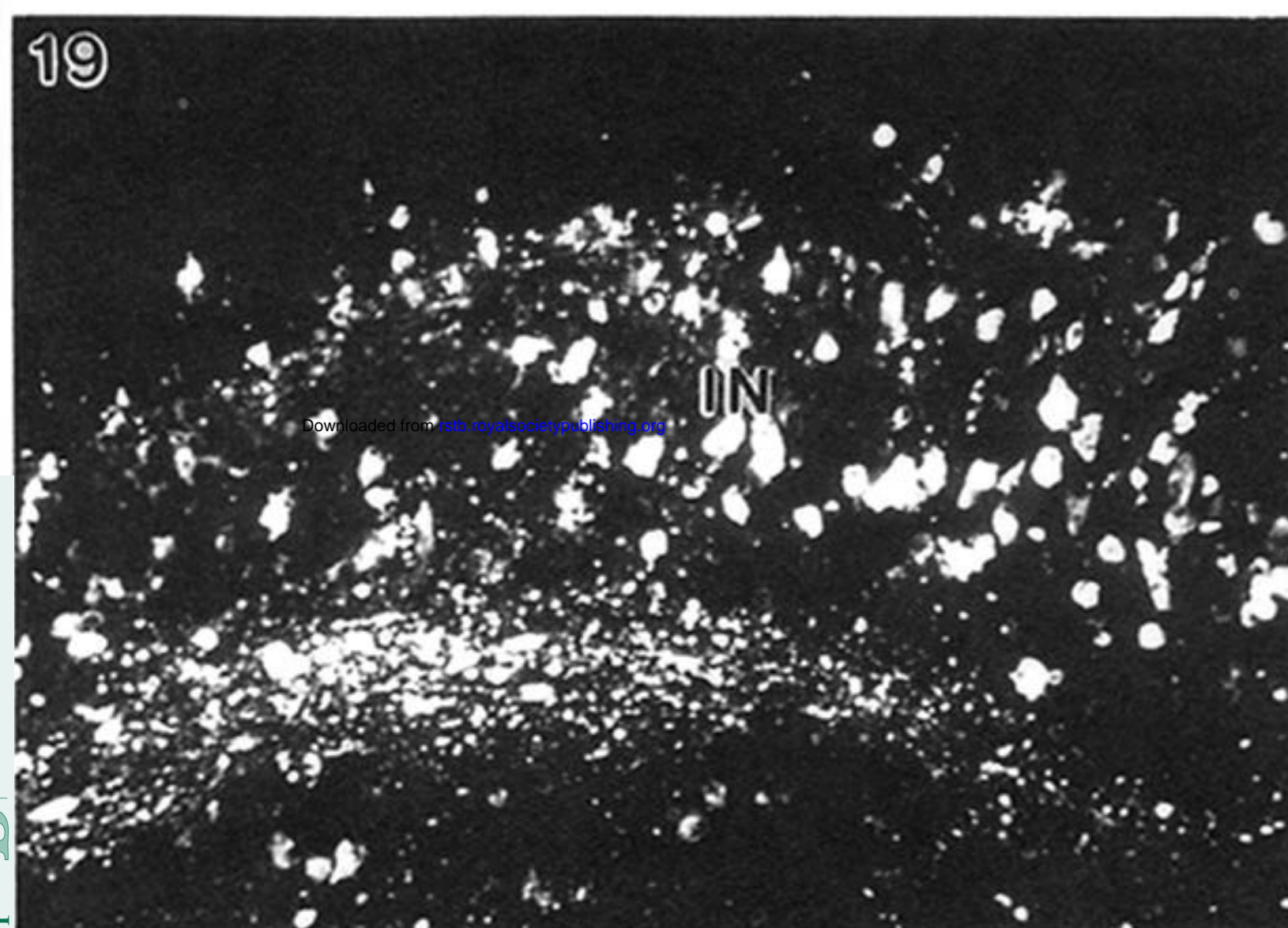
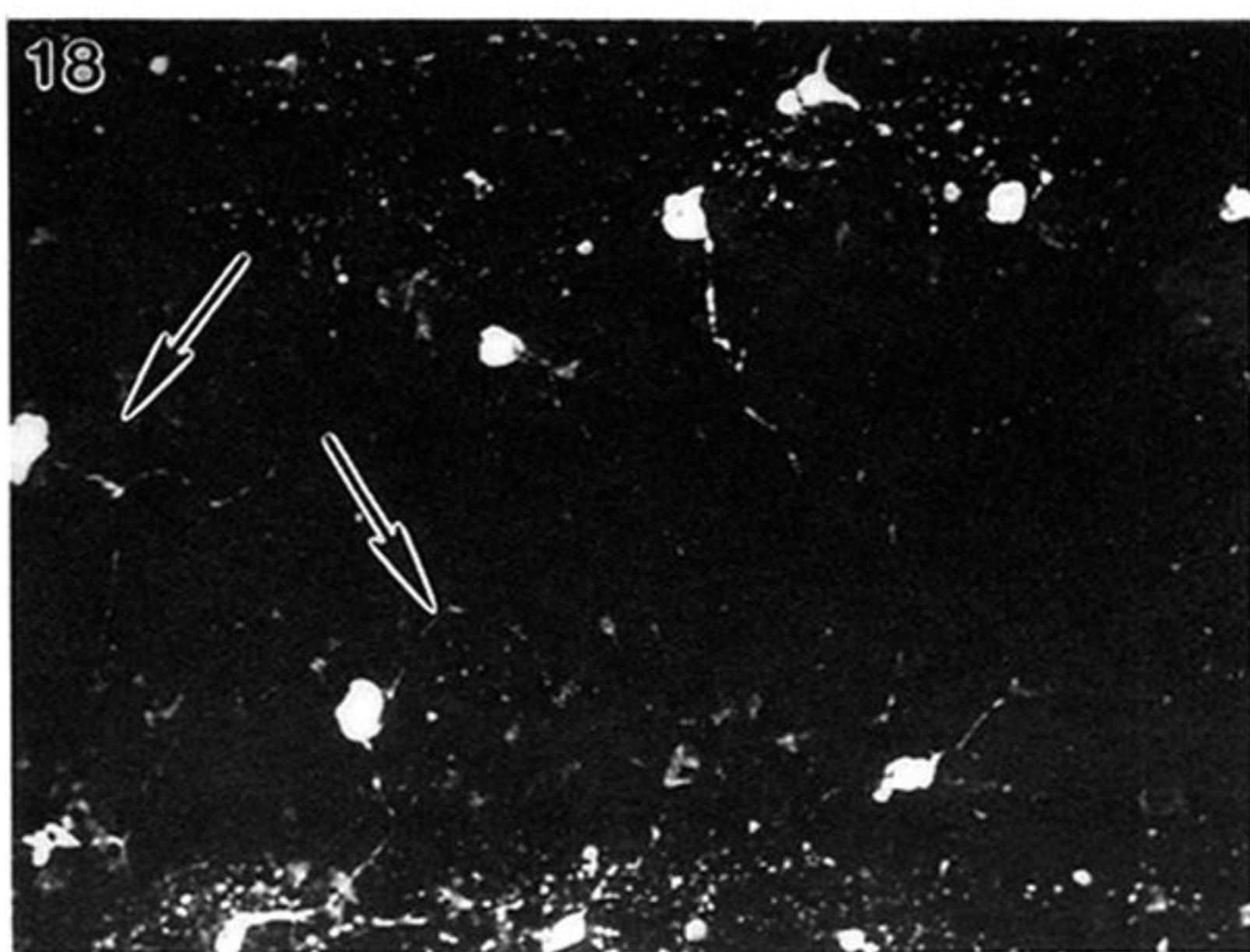
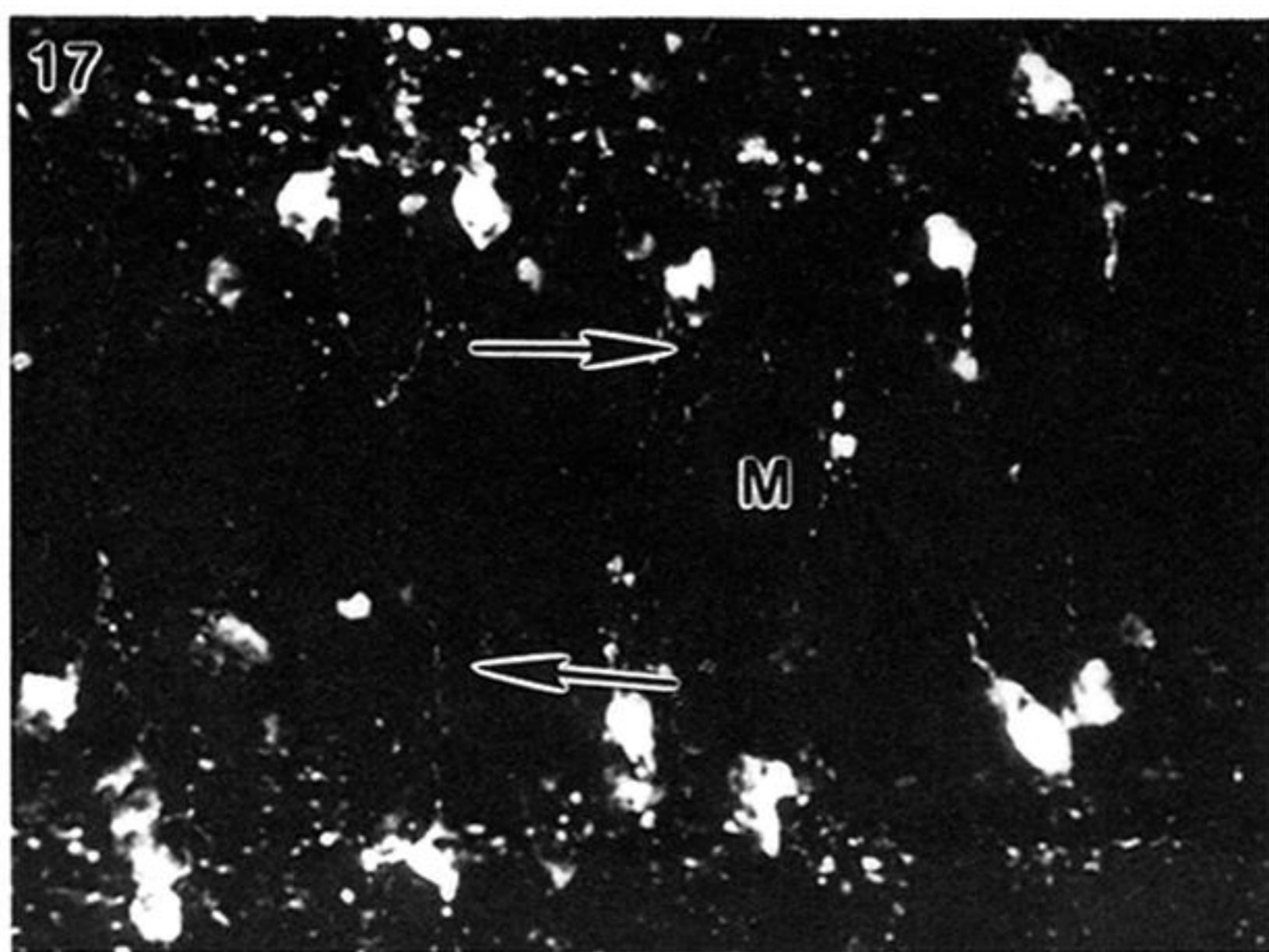
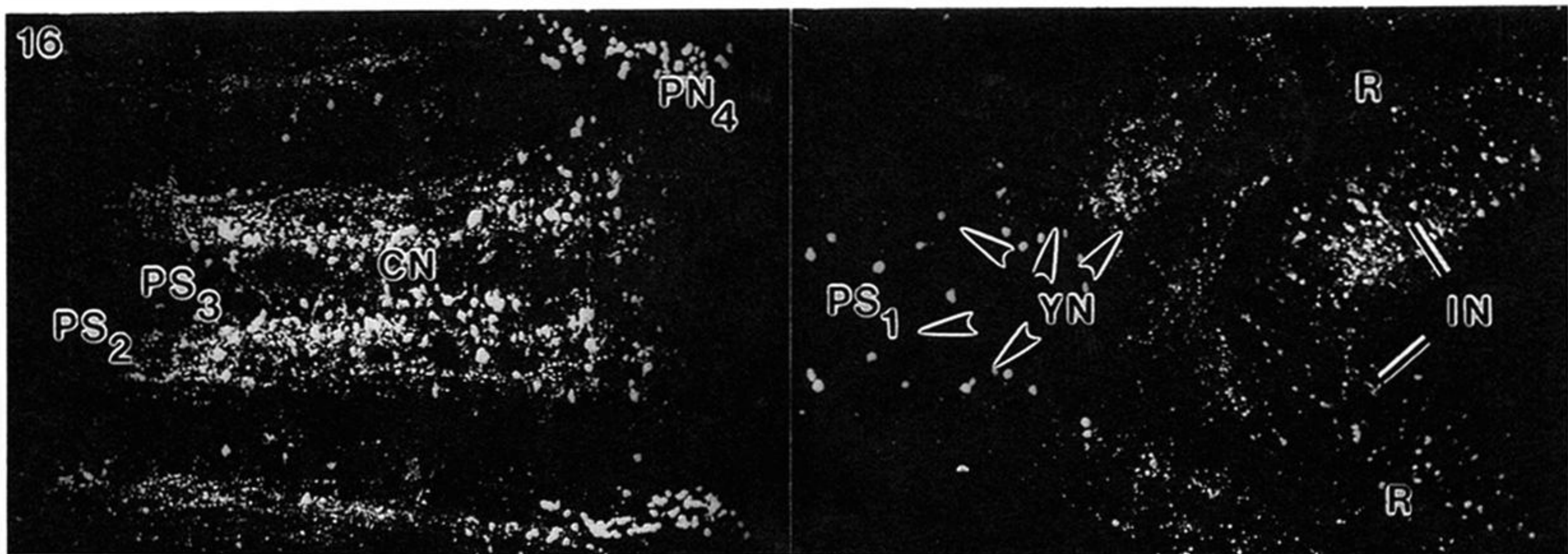
Received 31 March 1994; accepted 3 May 1994



Figures 3-9. For description see opposite.



Figures 10–14. For description see opposite.



Figures 16–20. S1-Li IR in the proximal segments of the radial nerve cord and the ring in *Ophiura ophiura*. All illustrations are whole mounts.

Figure 16. General view of the immunolabelling in the proximal segments and part of the ring. The second proximal segment (PS<sub>2</sub>) is characterized by a large population of small central monopolar neurons (CN) and an important group of peripheral neurons (PN<sub>4</sub>) in the interganglion. The first proximal segment (PS<sub>1</sub>) only contains a small group of Y-shaped neurons (YN). The inner edge of each ring branch (R) shows an important concentration of immunoreactive cell bodies (IN). (Magn. × 80.)

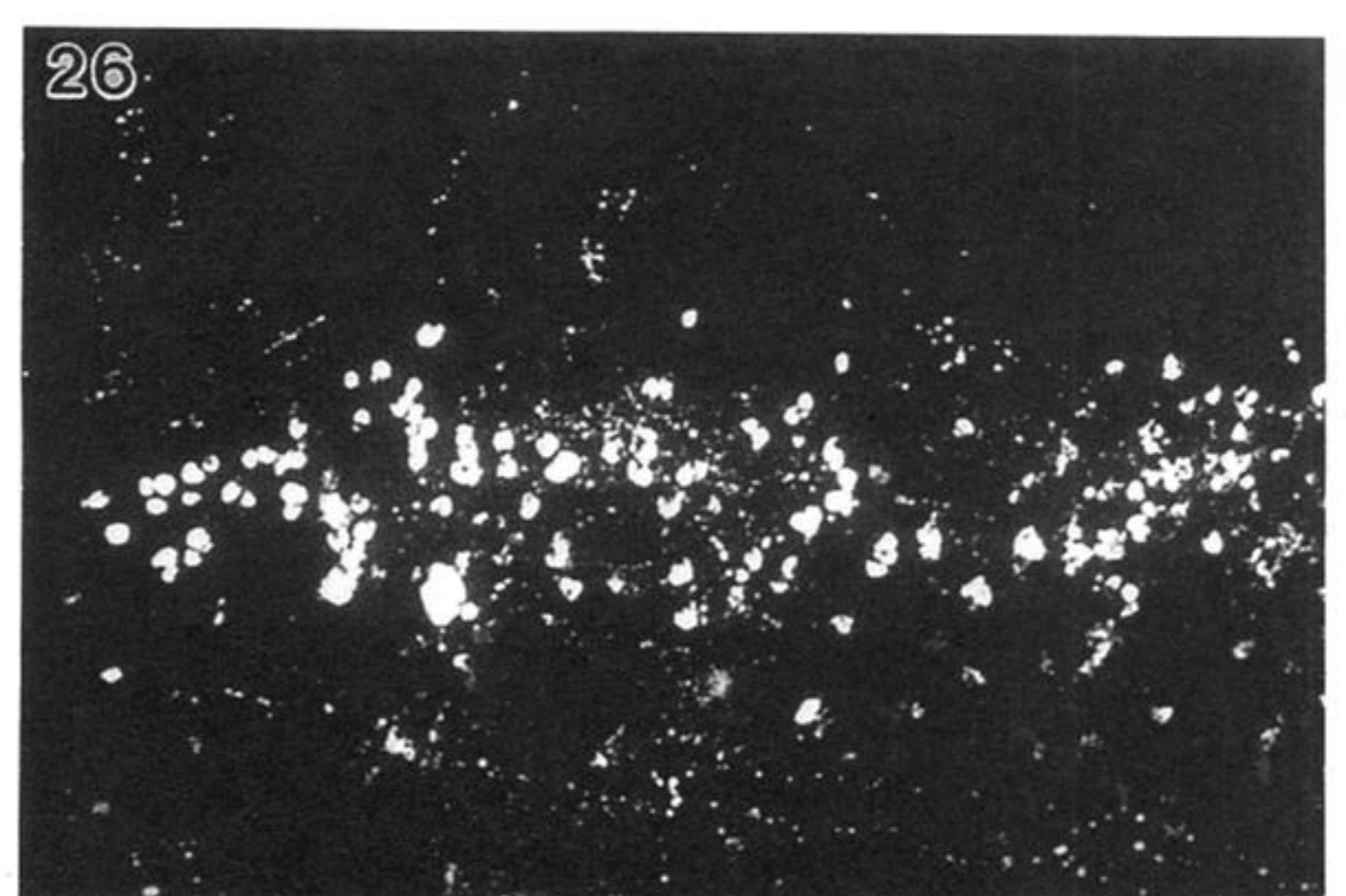
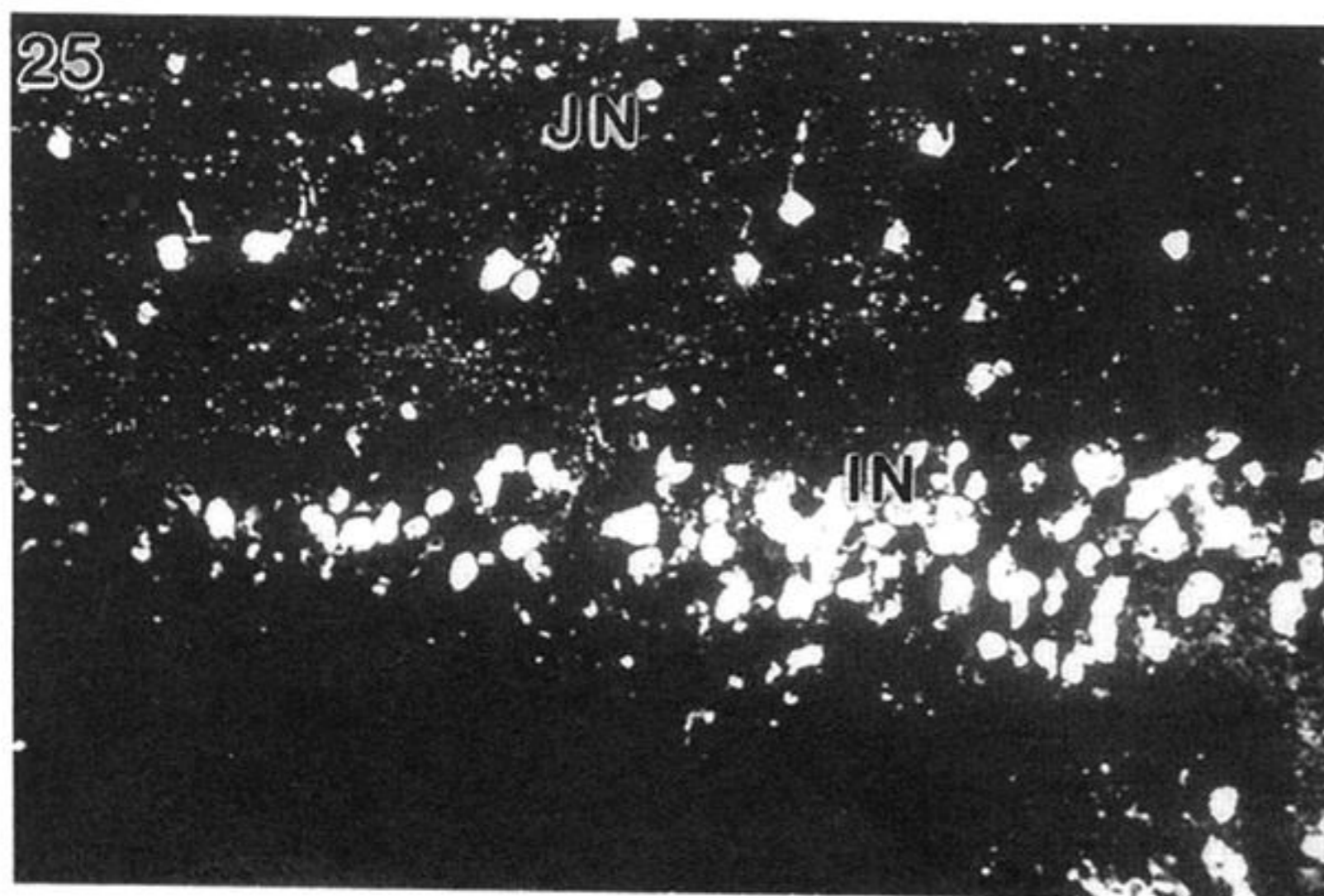
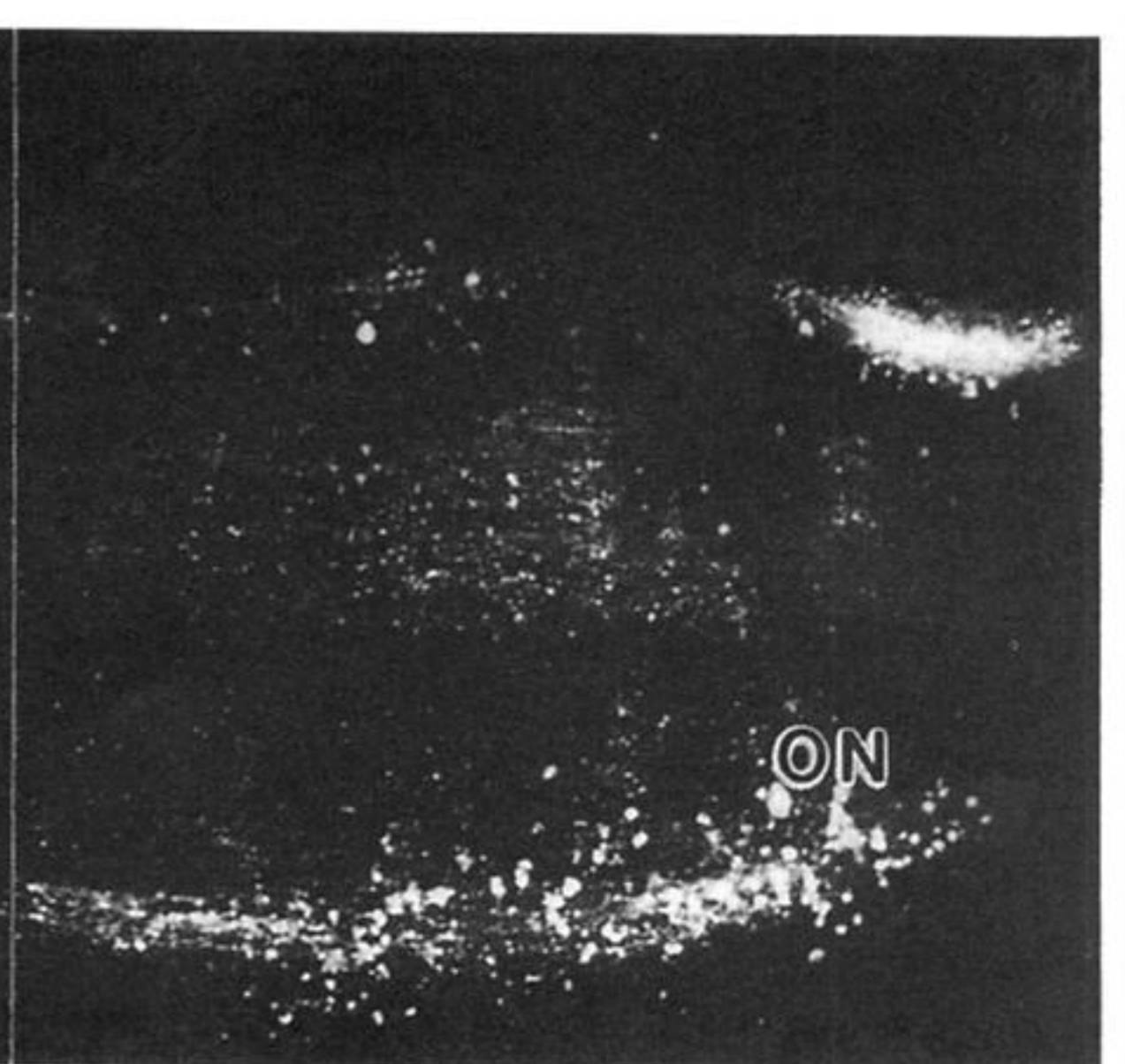
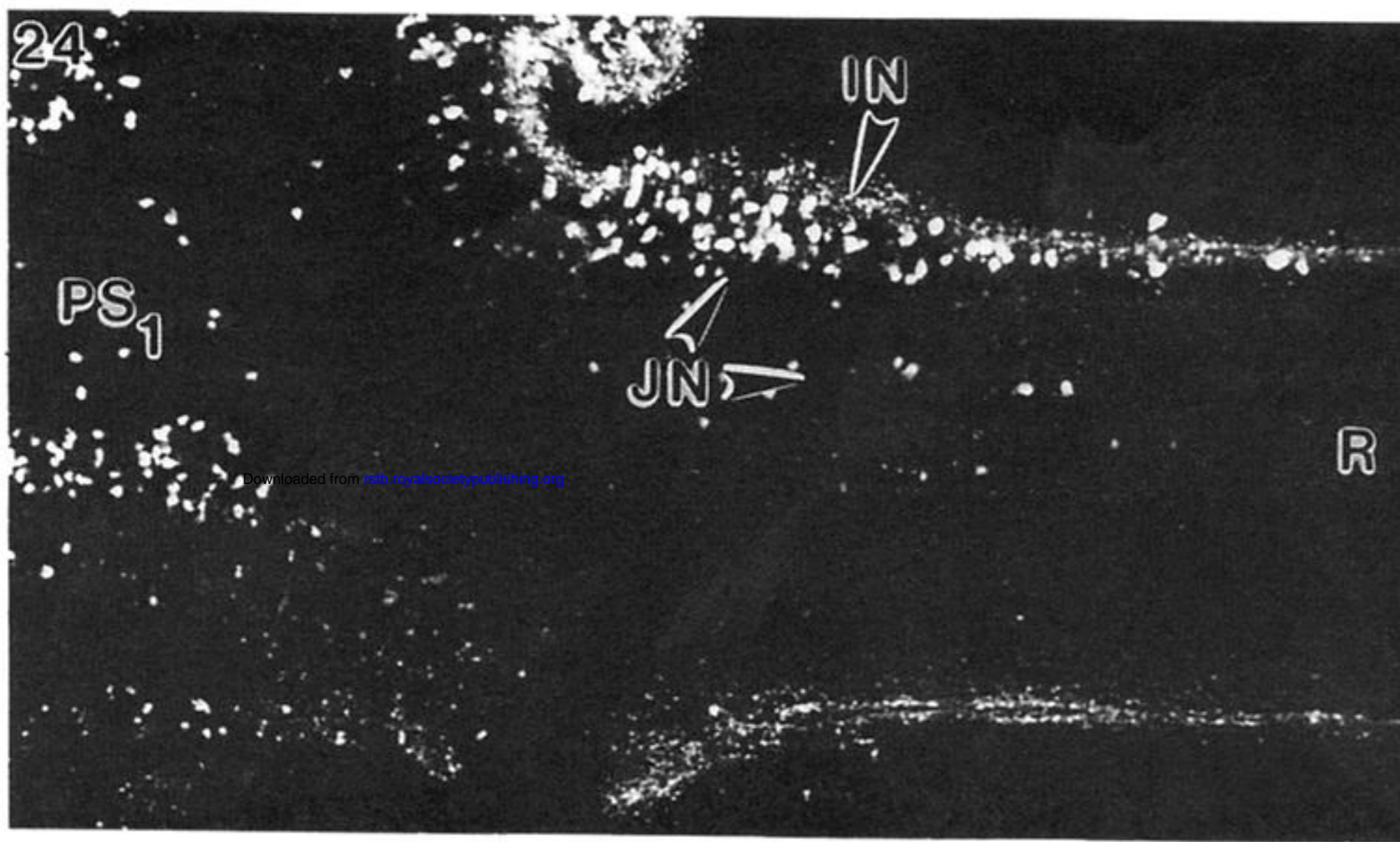
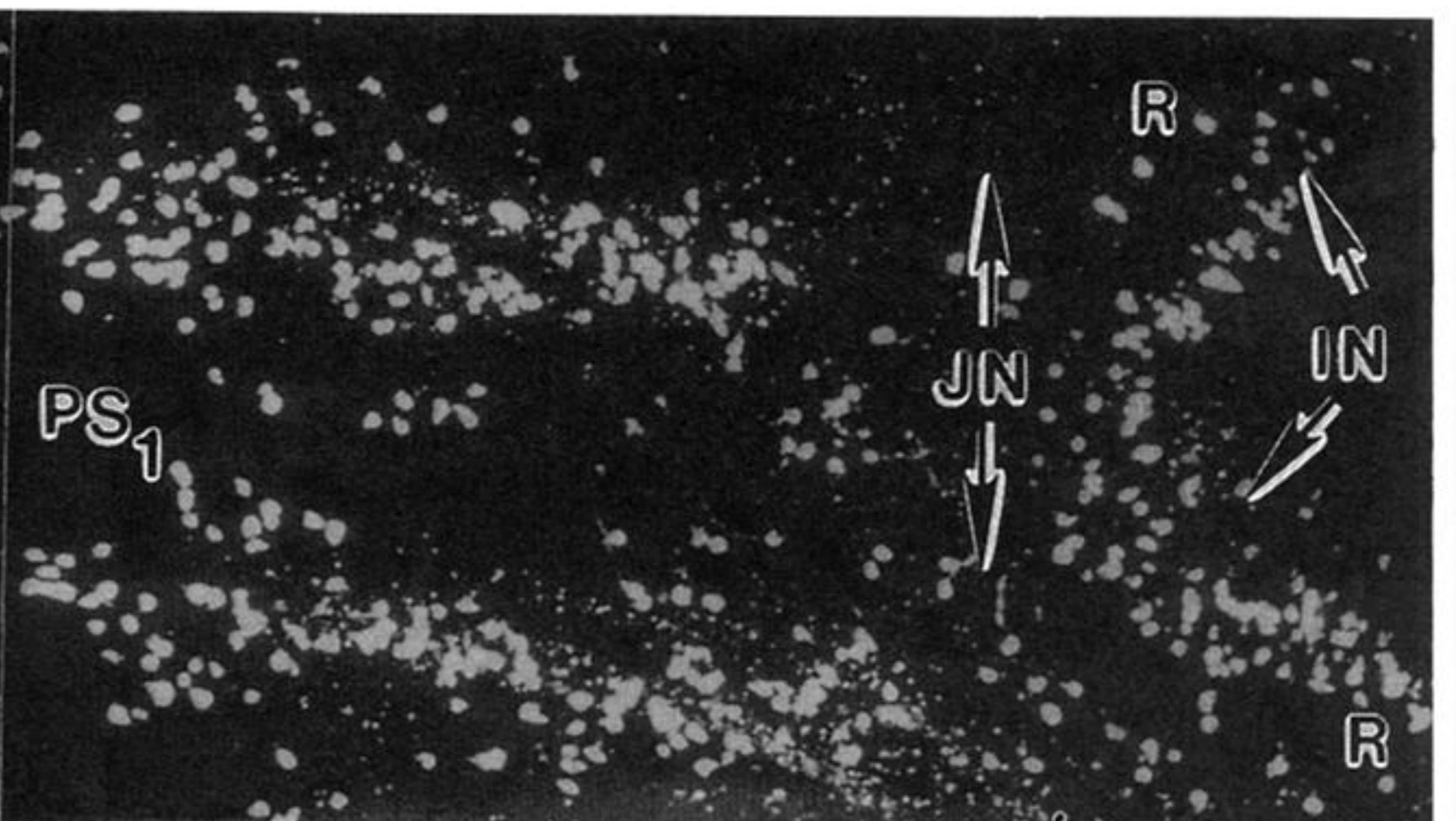
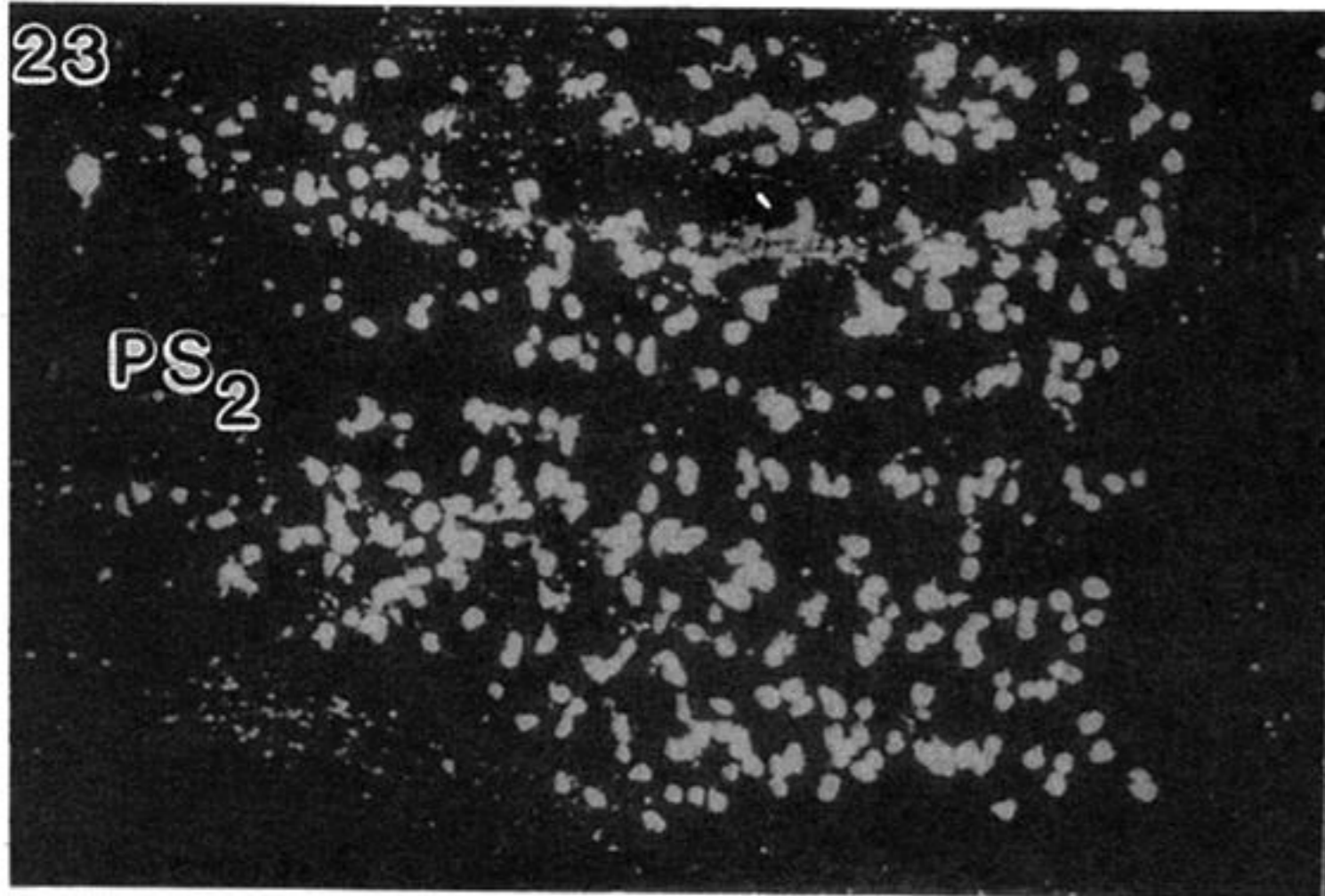
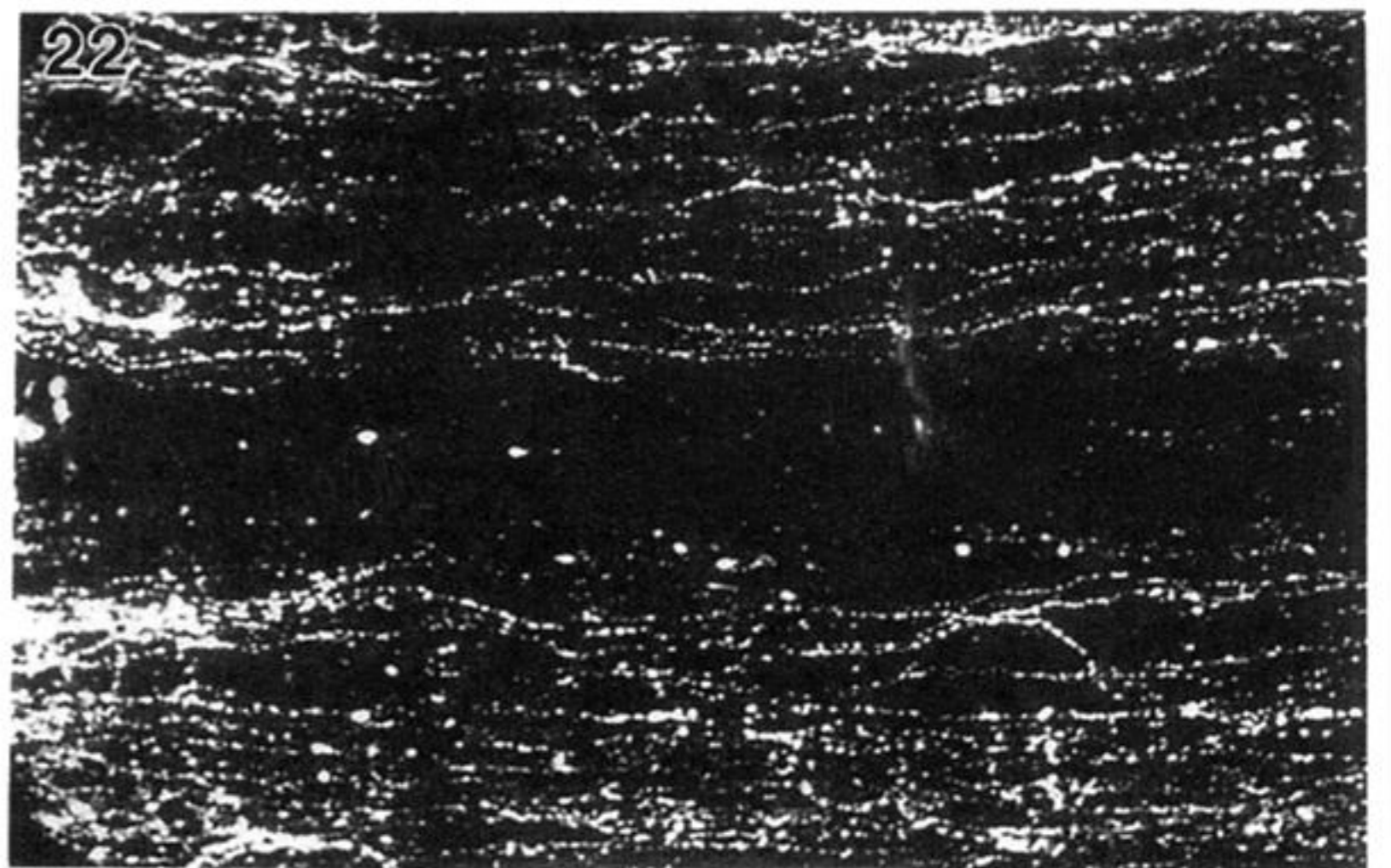
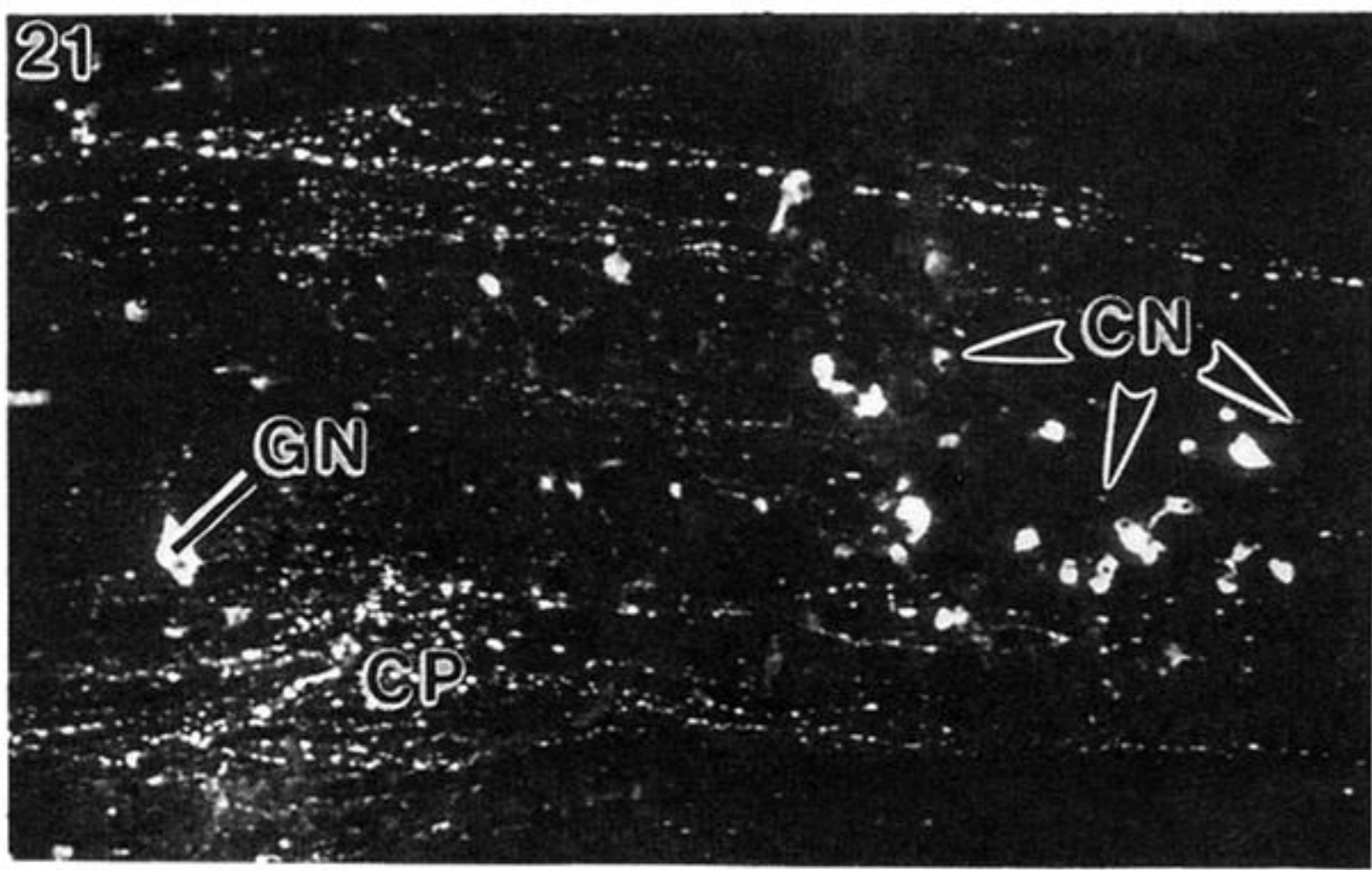
Figure 17. Central neurons of the second proximal segment sending monopolar processes (arrows) towards the nerve cord midline (M). (Magn. × 300.)

Figure 18. Y-shaped neurons (arrows) of the first proximal segment. (Magn. × 220.)

Figure 19. Immunoreactive neurons (IN) along the inner edge of a ring branch. (Magn. × 180.)

Figure 20. General view of the distal part of a ring branch. There are fibre plexuses running along the inner and outer edges (IP and OP, respectively) and centrally (CP). Ectoneural and hyponeural cell bodies (ON and HN, respectively) are detected along the outer edge of the ring branch. (Magn. × 100.)





Figures 21–26. For description see opposite.